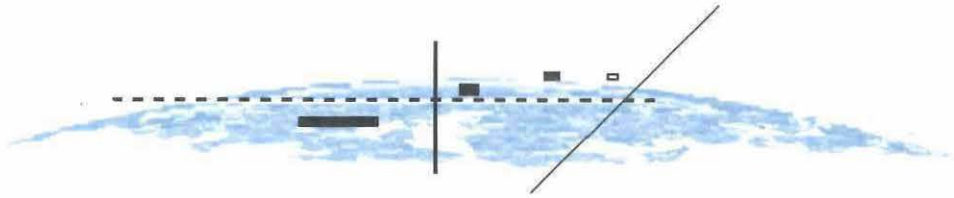

GeoForschungsZentrum Potsdam
STIFTUNG DES ÖFFENTLICHEN RECHTS

Jaroslav Klokočník,
Christoph Reigber, Peter Schwintzer,
Carl A. Wagner, Jan Kostelecký

Evaluation of pre-CHAMP Gravity Models GRIM5-S1 and GRIM5-C1 with Satellite Crossover Altimetry

Scientific Technical Report STR00/22

Jaroslav Klokočník,
Christoph Reigber, Peter Schwintzer,
Carl A. Wagner, Jan Kostelecký

Evaluation of pre-CHAMP Gravity Models GRIM5-S1 and GRIM5-C1 with Satellite Crossover Altimetry

DOI: http://doi.org/10.2312/GFZ.b103-00228
URN: urn:nbn:de:kobv:b103-00228

Imprint

GeoForschungsZentrum Potsdam
Telegrafenberg
D-14473 Potsdam

e-mail: postmaster@gfz-potsdam.de
www: http://www.gfz-potsdam.de

Printed in Potsdam/Germany
November 2000

Scientific Technical Report STR00/22

EVALUATION OF pre-CHAMP GRAVITY MODELS "GRIM5-S1" AND "GRIM5-C1" WITH SATELLITE CROSSOVER ALTIMETRY

Jaroslav Klokočník[1,2], Christoph Reigber[1], Peter Schwintzer[1], Carl A. Wagner[3], Jan Kostelecký[4]

[1] *GeoForschungsZentrum Potsdam (GFZ),*
Division "Kinematics and Dynamics of the Earth",
D-14473 Potsdam, Telegrafenberg A17, Germany
reigber@gfz-potsdam.de, psch@gfz-potsdam.de, klokoc@gfz-potsdam.de

[2] *Astronomical Institute of the Academy of Sciences of the Czech Republic*
CZ-251 65 Ondřejov Observatory, the Czech Republic
jklokocn@asu.cas.cz

[3] *NOAA/NESDIS Laboratory for Satellite Altimetry,*
1315 East-West Highway, Silver Spring, MD 20910, USA
carl.wagner@noaa.gov

[4] *Research Institute of Geodesy, Topography and Cartography,*
CZ-250 66 Zdiby 98, the Czech Republic
kost@fsv.cvut.cz, gope@asu.cas.cz, vugtk@ms.anet.cz

Summary. *The new GFZ/GRGS gravity field models GRIM5-S1 and C1, current initial models for the CHAMP mission, have been compared with other recent models (JGM 3, EGM 96) for radial accuracy (by means of latitude lumped coefficients) in computations on altimetry satellite orbits. The basis for accuracy judgements are extensive (multi-year) averages of crossover sea height differences from Geosat and ERS 1/2 missions. These data are fully independent of the data used to develop these gravity models. We tested how well these observed differences in all the world's oceans agree with projections of the same errors from the scaled covariance matrix of their harmonic geopotential coefficients. It was found that the tentative (model) scale factor of 5 for the formal standard deviations of the harmonic coefficients of the new GRIM fields is justified, i.e. the accuracy estimates, provided together with the geopotential coefficients, are realistic.*

Key words: gravity field models, accuracy assessment, satellite crossover altimetry.

Content

STR 00/22 German Research Centre for Geosciences
DOI: 10.2312/GFZ.b103-00228

1. Introduction

GRIM5-S1 (Biancale et al, 2000) and GRIM5-C1 (Gruber et al, 2000) are new gravity field models worked out in the frame of the German–French cooperation as a satellite-dynamics-only (S1) and a combined (C1) satellite-terrestrial gravity solution for use in the initial phase of the CHAMP mission. They replace GRIM4 (Schwintzer et al, 1997) and represent the current state-of-the-art in gravity field modelling. The new models were intensively tested and evaluated (Biancale et al, 2000 and Gruber et al, 2000) in the context of the gravity field determination process by using many model independent data and data products to prove their high accuracy and reliability. In this paper an additional almost global data set and a somewhat new test procedure, which can isolate errors in specific geopotential orders, is applied for a model quality check. The data are satellite altimeter cross-over residuals and the procedure makes use of the latitude lumped coefficients.

As both models are completely independent of satellite crossover altimetry, we can test them by this type of data, provided that a sufficiently accurate set of altimetry data is available. We make use of long-term averaged (over 1 year) single satellite crossovers *(SSC)*. Their original version was derived from NOAA or NASA Pathfinder data (Koblinsky et al 1999, http://neptune.gsfc.nasa.gov), at NOAA, with the gravity field model JGM 3. A table of all altimetry corrections is given in Klokočník et al (2000) or in Wagner et al (2000).

Crossover altimetry is ideal for testing satellite-only gravity models for two principal reasons: *(1)* The data is nearly global in extent and purely radial while normal tracking predominantly senses along-track perturbations of the field and only over limited areas, and *(2)* the data has not been used in the model development. Combined models (surface gravity data and tracking data), while often containing altimetry information either directly from their use as a type of tracking data type or indirectly through conversion to mean gravity anomalies, may also benefit from crossover tests which focus exclusively on just the radial perturbation of the satellite orbit.

The satellite data base of GRIM5-S1 and C1 is shown on Fig. 1. The expected radial accuracy (for S1), closely connected to the used satellites and tracking data and its accuracy and distribution, is shown in Fig. 2, plotted as a function of orbit inclination and selected altitudes. It was derived from the variance-covariance matrix of the harmonic coefficients of the model. This figure is reproduced from Biancale et al, (2000). The variance-covariance matrix used was already scaled by a factor of 5^2 (compared to the covariance matrix from the adjustment). This will be the case throughout this investigation, i.e. all standard deviations of the geopotential coefficients related to GRIM5s include the multiplication factor of 5. We see a typical local maxima of the radial error where fewer orbits exist at the lower inclinations and – to a lesser extent – for nearly polar prograde orbits. Fig. 3 (taken from Lemoine et al, 1998) compares the radial accuracy for several gravity models (before GRIM 5) to show the evolution and progress during the last decade.

CHAMP (Reigber et al., 2000) was successfully launched into an 87.3 deg inclined orbit. This is at a local maximum of the static-gravity field radial orbit error (Figs. 2 and 3). It is a good choice of inclination; for example, a 50% improvement of the radial error (at its altitude of 450 km) will not count just a few centimeters but will represent half a meter gain.

Information about the expected radial orbit accuracy shown by Figs 2 and 3 is useful and concise, it enables a simple and direct comparison for orbits with different inclinations (for a given altitude). We can extract from these curves the contribution of the data from the individual satellites to the gravity model. For example, observations of GFZ 1 and ERS 1, 2, SPOT 2, 3,

Westpac and STELLA satellites in GRIM5-S1 are responsible for the local minima of the radial error at $I = 50$ and 100 deg, respectively (Fig. 2). Observations of HILAT and RADCAL at $I =$ 83 - 95 deg contributed to a decrease of the radial error in EGM 96 in comparison with GRIM 5 and with the older JGM 2 or 3 models (Fig. 3), which do not include data from these satellites. Moreover, due to the symmetry of prograde and retrograde orbits around the pole, there are also "mirror" inclinations with additional local minima on orbits symmetrical to the pole and complementary to results at the original inclinations (e.g., $I = 130$ deg is a "mirror" to the 50 deg "original").

The ideal in geopotential development is to have not only low actual radial errors but to have them as "flat" as possible over "all" inclinations (flat curves for the radial error would be a result from a gravity model with homogeneous accuracy over all its spectral parts). But one can see that even the recent gravity field models (combination models inclusive) are still far from that ideal. A contribution of the satellite-to-satellite measurements from CHAMP is anticipated not only for its orbit inclination, i.e. mainly to cut the peak of the radial error at 80-90 deg (due to satellite dynamics), but also "generally" i.e. to reduce (partly) the radial accuracy also at other inclinations (due to continuous satellite-to-satellite tracking).

While the information on Figs. 2 and 3 is useful, it does not provide any insight into the geographical distribution of the radial error in latitude and longitude. This is accomplished in this study by using Rosborough's tranformation to project the GRIM5 variance-covariance matrices to yield expected errors of SSC geographically. But such information, while useful as an overview, says nothing about the spectral quality of the errors. Following the natural formulation of spherical harmonics, this "Rosborough spectrum" is most readily displayed by order in terms of so-called *latitude lumped coefficients (LLC)*.

The expected errors in the LLC will be propagated from the (scaled) variance-covariance matrix but also will be computed from the "observed" SSC, i.e. derived from independent altimetry data. Then, one can compare both quantities and, under certain conditions, one can calibrate the gravity field model's covariances to get an accuracy estimate closer to reality.

2. Methodology

2.1. Single Satellite Crossovers

We recall Rosborough's (1986) geographical representation of the radial error from which it is well known that each radial error consists of two components: the geographically correlated and the variable (anticorrelated) parts.

It is the geographically dependent (correlated) part of the radial error which is cancelled out (thus not observable) from the full radial error in altimeter crossover differences. This component has a comparable amplitude to the variable part of the radial error and cannot be neglected. Thus, even if we assess the variable part of an orbit radial error as negligible, the sea surface topography from averaged satellite altimetry could still be corrupted by substantial gravity induced orbit errors from the geographically correlated part. For the lowest orders, this part seems to dominate the total radial error (depending also on orbit inclination). Nevertheless, our tests of orbit-geopotential models with SSC's can still be expected to give a good indication of the overall radial performance of the model since the variable component is generally substantial as

STR 00/22 German Research Centre for Geosciences
DOI: 10.2312/GFZ.b103-00228

well. The geographically correlated error can never completely be eliminated using SSC information only. Its further reduction is possible only via a further general gravity field improvement.

There is another type of altimetry crossovers, between two distinct orbits (Dual Satellite Crossovers, *(DSC)*) which does invoke differences of the geographically correlated errors between the two orbits. While this has been a promising approach to address the full radial orbit error from gravity mismodelling, the use of such data for testing model errors is limited because of the increased media and sea surface errors, introduced by the two missions (compared to SSCs).

Recalling Rosborough (1986) again: for purely geopotential effects with respect to a single satellite with a nearly circular orbit (same semimajor axis and inclination), the SSC values, $\Delta X(\phi, \lambda)$, at position ϕ and λ (and in turn its errors), is free of the geographically dependent part $\Delta\gamma$ of the radial orbit component/error Δr, i.e.

$$\Delta X(\phi, \lambda) = \Delta r^A - \Delta r^D = 2\Delta\delta, \tag{1}$$

where A, D denote the *a*scending and *d*escending tracks (used for crossover computation), respectively, and $\Delta\delta$ is the variable component. [Note that even the "variable" component at a location belongs to the static gravity field (as the geographically correlated or mean part does), and is not time-variable at that location, but contrary to the mean part of opposite sign for ascending and descending tracks. The terms "mean" and "variable" were introduced by Rosborough, and we follow him. However, the term "variable" is sometimes replaced by "geographically anti-correlated"].

2.2. Latitude Lumped Coefficients

Latitude Lumped Coefficients (LLC) are linear combinations of the harmonic geopotential coefficients of different degrees l and the same order m, as sensed by the particular satellite. They provide information about the gravity model for separate orders over a wide range of latitudes (limit given by inclination of the satellite orbit).

LLCs were defined (for SSC) in Klokočník et al (1992) and applied to test previous calibrations of the gravity field models GEM T2 and JGM 2 (Wagner and Klokočník 1994; Wagner et al, 1994). Since that time the concept of LLC based on SSC has been extended to the dual-LLC, based on DSC (Wagner et al, 1997b). In this paper, we will use the single-LLC to show details in distribution of radial orbit error per order and latitude (Sect. 3.2.) and for the accuracy assessment of the GRIM5-S1 and C1 models (Sect. 5).

Following (Klokočník and Kobrle 1992, Klokočník et al 1992), for the SSCs we may write

$$\Delta X(\phi, \lambda) = \sum_{m=1}^{m=m_{max}} \left[C_m(\phi, a, I) \sin m\lambda + S_m(\phi, a, I) \cos m\lambda\right], \tag{2}$$

where $C_m(\phi, a, I), S_m(\phi, a, I)$ are the LLC, pertaining only to the variable part of the perturbations at a crossover point (Rosborough, 1986):

$$C_m = \sum_{l=m}^{l=lmax} 2Q^S_{lm} C_{lm} \qquad S_m = -\sum_{l=m}^{l=lmax} 2Q^S_{lm} S_{lm}, \tag{3}$$

I is the orbital inclination, a semimajor axis of satellite orbit, the Qs are the influence functions (Rosborough 1986) and ϕ is geocentric latitude. The harmonic geopotential coefficients C_{lm}, S_{lm} are fully normalized (in turn, the LLCs are also fully normalized and the inclination functions

inside the Q-functions too). For more details, more compact formulae for single and dual LLCs in "one", and formulae for the error propagating from the variance-covariance matrix to the LLC error, see Wagner et al (1997b).

2.3. Linear transfer of single satellite crossovers

Sea surface height estimates from precisely positioned altimetry satellites and the resulting SSC are our test data. The processing steps from precision orbit determination to sea surface heights and crossover values is complex and time consuming. Many corrections need to be introduced to the measured altimeter height to account for numerous delays and distortions in the signal due to wet and dry troposphere, ionosphere and sea state bias as well as a time variable ocean surface model from tides and atmospheric pressure apart from the gravitational impact on the satellite orbit. We generated SSC for Geosat (ERM plus GM missions), ERS 1 and 2 with software developed by Russ Agreen, Carl Wagner and others from NOAA, Silver Spring. Then, we generated long-term averages (more than 3 years) and standard deviations *(sd)* of the crossovers to reduce short term errors in the media models and seasonal variations of these, using only data in the same months of different years. The reference gravity field was always JGM 3 (Tapley et al, 1996). Details of these reductions are explained elsewhere (Klokočník et al, 1999, 2000, Wagner et al, 2000).

JGM 3-based SSC of ERS 1 and Geosat are shown in Fig. 4. These crossover values should be largely free of any "non-gravitational" effect, more precisely, almost all orbit effects others than from the static gravity field model, and all time varying altimetry delays and biases should be eliminated. We call such corrected SSC "crossover residuals", $\delta\Delta X$. But in reality, residual "non-gravitational" effects, including the impact from the absorbtion of orbit perturbations by empirically determined parameters (such as initial elements) in the determination process, still contaminate these data. (Concerning the empirical acceleration parameters used in precise orbit determination, we used a cut in perturbations with periods longer than is the arc lenght, see Klokočník et al, 1995a). We try to quantify these residual effects statistically (Sect. 4.1).

While the global *rms* values of the crossover residuals $\delta\Delta X$ (Figs. 4, 6 and 32) are typically a few centimeters to 10 cm, their formal errors (*sd*) are only around 1 cm, due to the long-term averaging and due to a large number (often hundreds) of measurements at the same location; these formal *sd* are shown on Figs. 4 e, f and 32 e.

In order to avoid a repetition of the whole processing, crossover residuals based on the GRIM5-S1 and C1 models are predicted (transformed) from the "true" crossover residual values by means of a linear transfer. In the linear transfer, the original orbit adjustment is kept unchanged but the harmonic geopotential coefficients of one gravity model are replaced by the coefficients of another model. For example, the crossover residuals $\delta\Delta X$ of the "new" field (GRIM5x) are estimated from the SSC based on the "old" model (JGM 3) and by the difference $\delta\Delta X_{new-old}$:

$$\delta\Delta X_{new} = \delta\Delta X_{old} - \delta\Delta X_{new-old}. \tag{4}$$

The difference is computed by Eq. 2, replacing the LLC values by their differences, which originate from the differences of the harmonic coefficients between these two gravity models. In this transformation, we cut all perturbations with excessive periods.

We performed various tests of the reliability of this linear transfer method to demonstrate that it is a good approximation to "real world". Some of these tests are shown in Figs. 22–25, Sect. 4.1.

STR 00/22 German Research Centre for Geosciences
DOI: 10.2312/GFZ.b103-00228

The results achieved by this transfer are the SSC GRIM5-S1 and C1 "predicted" residuals (Sect. 4.2.), shown on Fig. 4 for GRIM5-S1 and on Fig. 6 for GRIM5-C1, the former with a 4 day cut of orbit perturbations, the latter with a 1.3 day cut (see also Sect. 5.2).

2.4. Calibration

The tools to calibrate a gravity field model by means of independent altimetry data are now at hand: (1) we have observed or predicted crossover residuals of SSC, representing an accurate data set apparently dominated by the static gravity field mismodeling only, and (2) we have the variance-covariance matrix of the harmonic coefficients of that gravity field which was used to compute the orbit of these altimeter satellites and their crossover residuals. We want to check the applied variance-covariance matrix to get a realistic error estimate for the gravity field coefficients.

From the given observed or predicted crossover residuals $\delta\Delta X$ available over all latitudes and longitudes, we compute (by a least squares adjustment, LSE), order by order, the "observed" or "predicted" LLC discrepancies using (2) as the observation equation. Given are now $\delta\Delta X$, and computed are dC_m and dS_m, by replacing ΔX and $(C,S)_{lm}$ in eqs. 2 and 3 accordingly.

From the given variance-covariance matrix, we compute the LLC standard deviations (the formulae are in Wagner et al, 1997a,b) for each order and latitudinal belt separately. We call the result "projected LLC errors".

Finally, we compare the "observed/predicted" and "projected" error quantities and assess their difference statistically to arrive at a judgement of the scale factor for the covariance matrix of the model to be tested.

The LLC discrepancies derived from $\delta\Delta X$ are shown on Figs. 27 and 29 for ERS 1 and Geosat and will be used in Sect. 5.1. Those for ERS 1/2 combined set are given in Fig. 33d (Sect. 5.2.).

The LLC errors projected from the covariances of the harmonic geopotential coefficients of JGM 3, EGM 96, GRIM5-S1 and GRIM5-C1 are shown (for a wider comparison) in Figs. 17–21, for ERS 1, Geosat, TOPEX/Poseidon, CHAMP, and GFZ 1, respectively (further details in Sects. 3.2. and 5.).

This method has already been used to calibrate GEM T2 (Wagner and Klokočník, 1994) from Geosat and ERS 1 crossover altimetry using original crossover observations and JGM 2 and JGM 3 with LLC derived from such observations (Klokočník et al, 1999). Here we just note that in the adjustment of the "observed" LLC discrepancies from the crossover residuals, it is necessary to account for continents. In the LSE, the equation system is stabilized by using zero as a pseudo-observation for the solved-for parameters dC_m, dS_m (weighted by adopting a white noise assumption). In particular, from Geosat and ERS 1 analyses, we found that using a generous 80 cm as a priori white noise power for all latitudes yielded acceptable solutions even for the most poorly represented northern latitudinal "continental" bands. We distributed this power evenly among the 60 orders "resolved" for each band (the Nyquist limit for the bins spaced 3 degrees in longitude). By this approach, no artificial crossover residuals need to be introduced over land to obtain a solution. We tested the adjustment by LSE with and without eliminating the local 1 cpr empirical correction.

The test with LLC is always stronger for the southern hemisphere (less land areas). This fact is described by a larger scatter of the "observed" LLC discrepancies in the northern hemisphere (see Figs. 27 and 29), mainly for GRIM5-C1. For a more objective accuracy assessment (Sect. 5), we rejected the majority of northern latitudes (and the most southern bands, too), and finally, we used the LLC in the latitudinal range from 20 to -60 deg (more details are in Sect. 5).

2.5. Statistics

The method here outlined has already been used to study residual errors in altimetry (Klokočník et al., 2000). It is considered to be a subsidiary tool for identification of possible systematic errors in the crossover data and is used here in the frame of accuracy assessment of gravity field models.

Let us consider SSC residuals $\delta\Delta X$, based on a gravity model, and their standard deviations (formal *sd*) derived from point and time averaging, $s_{\delta\Delta X}$, and the SSC error s_{SSC} as projected from the relevant covariance matrix of the harmonic coefficients of the model (with a scale factor). Consider also an additional error source from non-gravitational effects in altimetry data, mostly from imperfect altimetry corrections, s_{ng}. Let us compute the total error estimate s_δ as

$$s_\delta = \sqrt{s^2_{\delta\Delta X} + s^2_{SSC} + s^2_{ng}}. \tag{5}$$

The ratio

$$r = \frac{\delta\Delta X}{s_\delta} \tag{6}$$

then should belong to the Student distribution. To investigate the null hypothesis, i.e. expectation value of $\delta\Delta X = 0$, the ratio

$$r_t = \frac{|\delta\Delta X|}{t_{\alpha,n}\ s_\delta}, \tag{7}$$

is plotted, with $t_{\alpha,n}$ being the significance level of the Student distribution for risk α=1% and n the degree of freedom (corresponds to number of crossover residuals in the given location).

The Student distribution depends on the sample number n. For higher n, there is practically no difference to the normal distribution. For n below about 10 points, the statistics is not conclusive for our purpose.

The ratio r_t lower than 1 means that the measured SSC residual is random (accounting for its estimated accuracy), while r_t larger than 1 means that the SSC exhibit a systematic effect (not covered by the covariance matrix and by the formal errors of the SSC). It is also possible to say that $r_t < 1$ means that we accept the null hypothesis, while in the opposite case that we reject it. To adopt an increase or decrease of the scale factor, we need more such results from different orbits (but we have only two, ERS and Geosat). More discussion is in Sect. 5.

The results of Students statistics are shown on Figs. 26a-e, 33a for ERS 1 and Geosat and on Fig. 33b for data combined from ERS 1 and 2. Values $r_t < 1$ are plotted by blue color, while $r_t \geq 1$ are in yellow or red. So, the yellow or red colors indicate that the SSC residuals contain systematic effects or that the variance estimation is too optimistic. On the other hand, if these colors are missing, the variance estimate may be too pessimistic. The problem is that we work with a geographical representation (with latitude and longitude); it is difficult to decide whether

STR 00/22 German Research Centre for Geosciences
DOI: 10.2312/GFZ.b103-00228

"yellow and red prevails". We accepted the following rule: if there are regular patterns, repeated often over the globe, with $r_t \geq 1$, we conclude that systematic effects occur (for the relevant orbit and gravity model), i.e. we reject the null hypothesis.

3. GRIM5-S1 and GRIM5-C1 among other gravity models

3.1. Propagation of variance-covariance matrices of JGM 3, GRIM5-S1, and GRIM5-C1 to radial orbit errors and its components

The JGM 3 global gravity field model (Tapley et al, 1996) is for us a "starting model" to generate GRIM5-S1, C1-predicted SSC residuals. So we need to know the radial error (and errors of its components, according to Rosborough) and the LLC errors projected (or propagated) from the JGM 3's calibrated variance-covariance matrix of the harmonic geopotential coefficients, for a comparison. In the case of GRIM5-S1 and C1 models, the preliminary, already applied scale factor for the their variance-covariance matrices is 5^2.

We present the radial orbit errors predicted for the ascending and descending track, the geographically correlated part $\Delta\gamma$ and the variable part $\Delta\delta$ of the radial error for both ERS 1 and Geosat with JGM 3, GRIM5-S1, and GRIM5-C1 variance-covariances to degree and order 70x70 on Figs. 7a,b,c,d – 12a,b,c,d always with a 4 day period cut of orbit perturbations. From a set of many other computations, we choose similar plots for CHAMP with JGM 3 (Fig. 13), GRIM5-S1 (Fig. 14) and with GRIM5-C1 (Fig. 15). A comparison with other gravity models can be found e.g. in Klokočník et al (1995a, 1996 or 1998).

The orbit perturbations longer than 4 days for ERS 1, Geosat, CHAMP, GFZ 1 and 10 days for TOPEX/Poseidon are cut by a filter in the projection software. We will see later however that there are some reasons to cut alternatively at about 1 day.

Results. Let us compare the projected errors with both models. There is an excess of satellite observations at the inclination of ERS-type orbits in GRIM5-S1 and C1 compared to JGM 3 (ERS 1, 2, SPOT 2, 3, Stella and Westpac in GRIM5s, but there is only SPOT 2 in JGM 3). Thus, for ERS 1 (Figs. 8 and 9), GRIM5-S1 and C1 yield smaller SSC errors than JGM 3 (Fig. 7). The remaining resonant peaks due to the shallow resonances can be removed (not shown) by cutting the perturbations at 1.3 days (or near this limit) instead of at 4 or 10 days. When cutting at, say, 300 days, (not shown), the long-periodic terms are added and create high "walls" at the shallow resonances. In general, the cut should correspond to the lenght of the arc in orbit determination. Thus, we prefer a 4 day cut for all but T/P (10 d), but sometimes (see below), we have to use a shorter one.

From Figs. 7–9 we see that also the geographical distribution of the errors is different for these different gravity models. The errors from the JGM 3 variance-covariance projection are less variable with latitude or longitude than those from GRIM5-S1. Recall that GRIM5-S1 is a satellite-only model, so some areas are less perfectly covered by data than in a comparable combination solution (C1 and JGM 3). This may explain the observed higher geographic variability of the projected errors; correlations between GRIM5-S1 coefficients are larger than in the combination solutions JGM 3 and GRIM5-C1. We compare the satellite-only model with the combined solutions with special care.

For Geosat (Figs. 10–12), however, the errors are significantly higher with GRIM5-S1 (and also with GRIM5-C1!) than with JGM 3. The reason is that there are only about two months of Geosat tracking data in the new GRIM5s. It explains the difference between Fig. 10 and 11. JGM 3 also benefits from extensive marine gravity anomalies derived largely from Geosat altimetry.

For the CHAMP orbit (Figs. 13–15), a large zonal signal is seen in all components of the radial error for all gravity models compared; variations with latitude dominate variations with longitude. It is an inherent nature for nearly polar orbits. JGM 3 performs slighly better for the CHAMP orbit than GRIM5-S1 or C1.

Usually the error in $\Delta\gamma$ is higher than in $\Delta\delta$, but the inclination of CHAMP provides an exception. All errors for CHAMP have a significantly "zonal" character, although (as always) all variance-covariance terms are used (never only the variances although it may be tempting to simplify the computations).

One can conclude from the geographical distribution of the radial errors that geopotential model errors project in a highly selective way to satellite orbits. In general, the contributions of errors of harmonics of different degrees and orders to the total radial error is not uniform. It strongly depends on orbit inclination and height. Thus, we usually have higher propagated errors due to resonant terms and the lowest order harmonics for orbits not well represented in the model. It can happen that the total error is created in fact by errors in just a few poorly modelled harmonics only. To get a deeper insight into this problem, we need to study variance-covariance projections for the spectrum of LLC errors.

3.2. Propagation of variance-covariance matrices of JGM 3, EGM 96, GRIM5-S1 and GRIM5-C1 to latitude lumped coefficient errors

We work again with the scale factor 5^2 for the GRIM5s variance-covariance matrices and with given calibrated variance-covariance matrices of the other models. We make use of the power of errors in C_m and S_m, i.e. root sum of squares (rss) of both C, S components.

The powers of latitude lumped coefficient errors, as projected from the covariance matrices of JGM 3, EGM 96, GRIM5-S1, and GRIM5-C1 (again to degree and order 70x70, and usually with the 4 day cut of orbit perturbations) are shown on Figs. 16, for an introduction. They are shown again on Figs. 17, 18, and 21 for ERS 1, Geosat, and TOPEX/Poseidon, and in addition on Figs. 19 and 20 for the non-altimetric missions CHAMP and GFZ 1, respectively. Note that two different directions of 3D projections are used on Fig. 16 as we want to show also the information hidden behind the "walls" of big power signals at selected orders. Note also different scales on the z-axis for Figs. 17 and 18 (ERS 1 and Geosat), for Figs. 19 and 20 (the low orbits of CHAMP and GFZ 1), and for Fig. 21 (T/P).

Results. LLCs unveil the selective nature of orbit inaccuracy due to the geopotential mismodelling over a wide range of latitudes and orders. Typically we find: (1) the largest errors are from the resonant and the lowest orders $m = 1$–4, (2) the higher the latitude and order, the higher the variability of the LLC error with latitude. (3) only a few orders dominate the radial error (often those from shallow resonances). These facts – while anticipated from the simplified approach (Figs. 2–3) – could not be quantified from it nor from the traditional Rosborough's geographic projections (Figs. 7–15).

STR 00/22 German Research Centre for Geosciences
DOI: 10.2312/GFZ.b103-00228

For ERS 1 (Fig. 17), the LLC errors are slighlty higher with GRIM5-S1 for the few lowest and resonant orders (m = 2, 4, 14, ...) than with JGM 3 variance-covariances. For the majority of the remaining orders however, the opposite is true, although the signal is small everywhere (below 1 cm, compare to Figs. 7–8). The total radial error for ERS 1 with GRIM5-S1, and namely C1, is smaller than with JGM 3 (compare Figs. 8, 9 to Fig. 7). The LLC errors disclose the contribution order by order to the total error. But this result depends also on a different filtering of orbit perturbations during the orbit determination and different manipulation with the empirical acceleration terms like 1 cpr (cycle per revolutions) in JGM 3 and GRIM5-S1, C1 (which shall be reflected in the variance-covariance matrices).

For Geosat (Fig. 18), GRIM5-S1, C1 perform obviously poorer than JGM 3 (as we have discussed and seen from Figs. 10–12), especially for the lowest and resonant orders. This is, as mentioned above, due to the limited amount of observations of Geosat in GRIM5s. On the contrary, with an inclusion of more Geosat data (although being "old"), and properly weighted, the new GRIM models could be improved to show significantly deeper local minima of the radial error in the vicinity of I = 108 and 72 deg.

For the low orbit of CHAMP (Fig. 19), the contribution of the lower order errors is surprisingly small in all 4 variance-covariance matrices compared, while errors due to the resonant harmonics prevail and are huge (Fig. 19). But recall that we applied again the 4 day cut and that many shallow resonant terms have periods below this limit. For a 1 day cut, for example, these peaks at the shallow resonances partly dissapear. The significantly lower altitude of CHAMP contributes to this turn-around as the higher (resonant) orders are enhanced relative the lower one's when the altitude is reduced. JGM 3 brings larger errors for the 15th and 16th orders than GRIM5-S1 or C1, but the opposite is true for order 31. The best behaviour is shown for EGM 96 (Lemoine et al, 1998) due to additional data at the polar orbits in comparison with JGM 3 (Klokočník et al, 1998, see Fig. 1 on p. 223, Fig. 6 on p. 230). Note that also the 61st order is still sensitive (LLC error up to 50 cm) and that a truncation at degree and order 70 is not sufficient (due to the low orbit of CHAMP) to represent the complete signal of LLC errors.

The dramatic impact of GFZ1 data (I = 51.6 deg) included in GRIM5-S1 and C1 is shown in Fig. 20. For this inclination and low altitude, the GRIM5s evidently win over JGM 3 and EGM 96. While the LLC errors for the main resonant orders are sometimes above 1 meter with the JGM 3 calibrated variance-covariances, they are roughly 10 times lower with the GRIM5-S1 or C1 scaled variance-covariances. This is due to the fact that the new GRIMs contain several years of GFZ 1 data whereas JGM 3 or EGM 96 do not.

LLC errors for TOPEX/Poseidon (10 day cut) are shown on Fig. 21. Note the change of scale on z-axis. GRIM5-S1 and C1 perform very well for this orbit, better than JGM 3 and certainly better than EGM 96. The last two models were already compared for the T/P orbit (Klokočník et al, 1998); while traditional orbit tests indicate that EGM 96 performs a bit better on ordinary T/P tracking, than JGM 3, the LLC errors on Fig. 21 tell the true story: EGM 96 is worse for lower non-resonant orders than JGM 3, while the resonant peaks are smaller than in JGM 3. In the total radial orbit error, EGM 96 then looks better. This is a good example how traditional orbit tests, so widely in use, neglect the important order-contributions to the radial error, and may be misleading. Slightly different filtering of orbit perturbations with periods somewhere between 1 and 10 days and various empirical terms in the orbit adjustment between two models may mask the actual orbit accuracy from the given geopotential model. Thanks to the LLC error estimates, we have a better insight into the accuracy structure.

4. Single-satellite crossovers as input data

4.1. Test of linear transfer of satellite crossovers

We have performed a number of tests to verify the empirical method of linear transfer of original SSC residuals based on one gravity model, to predict SSC residuals based on another geopotential. Recall (Sect. 2.3.) that the transfer only replaces the harmonic geopotential coefficients and makes an assumption about the effects of gravitational perturbations in the original orbit. A few examples of these tests are shown in Figs. 22–25. These tests represent an important prerequisite for the interpretation of the transformed GRIM5-S1 and C1 SSC, used later (Sect. 5) for a check of the variance-covariance scaling.

Fig. 22 shows a test of the transfer from DGM-E04 (Scharroo and Visser, 1998) SSC originals (Fig. 22a) to JGM 3-predicted SSCs (Fig. 22c). But we have already the "observed" JGM 3-based SSCs (Fig. 22b) from NOAA data available (Klokočník et al, 1999), so we can compare the prediction with the real data, albeit the DGM and NOAA data used different backround media corrections and may have used different empirical orbit models in their derivation. The comparisoon is shown on Fig. 22d. We see the prediction is successful, *rms* of the difference between the original and predicted SSC being only about 2 cm in contrast to the amplitude of the signal of the SSC residuals being mostly between -20 and +20 cm. But there is also an unexplained systematic increase of the difference in the Indian ocean (Fig. 22d). Note that the transfer is done with a 4 day cut of orbit perturbations (it means that the perturbations with periods longer than 4 days are simply omitted).

Fig. 23 shows a test of the transfer for the orbit of Geosat (again with a 4 day cut), from earlier JGM 2-basis SSC observations to JGM 3. Again, we already know the result (i.e. we have "true" JGM 3-based observed SSC residuals). This time, Fig. 23d displays the difference between the JGM 3 based originally observed residuals and JGM 3 predicted SSC values. We see nearly no systematic effect over the globe, but strips or belts of larger differences are running along the orbit. They come from the 4 day cut which is not able to eliminate the influence of the shallow 14th order (and related) resonant terms. These terms have periods mostly between 1 and 4 days. We saw similar patterns in the predicted SSC residuals in Fig. 4.

The problem of filtering out long-wavelength orbit perturbations may degrade the transfer result. Thus, we experimentally found a limit of 1.3 days, where the effect of these artefacts is the smallest. For an even shorter cut, the differences (original-predicted) begin to increase again. Figures 24 and 25 indicate the role of filtering. Fig. 24 compares the 4 day and 1.3 day filter for the predicted ERS 1 SSC residuals, and Fig. 25 shows a similar example for Geosat. In both cases, the "resonant" belts mostly dissapear when we apply the 1.3 day cut.

The better fitting shorter cut (1.3 vs 4 days) is a strong indication that the emprical 1 cpr terms used in the orbit models for Geosat and ERS 1 to absorb along-track errors in their trajectories (recomputed roughly every day) has effectively absorbed important orbit-geopotential error in the radial direction as well. The resonant effects presented in the difference of the two orbit-geopotential models are filtered out by the 1.3 day cut in the transfer model analogous to the way they are actually filtered by the empirical terms in the orbit determination process which is background to the "observed" SSC differences. Note that while Fig. 24 has *rms* value of the remaining residuals of about 2 cm, in Fig. 25 we show a dimensionless weighted *rms*, computed as the rms of the SSC residuals divided by their formal *sd*.

STR 00/22 German Research Centre for Geosciences
DOI: 10.2312/GFZ.b103-00228

We are aware that the actual, "true" data (the SSC residuals directly from observations) would be better and safer for the calibration than the residuals only predicted or transformed by the gravity field transfer (with no change in orbit). However, the procedure of computing the SSC from observations is time consuming and complicated. With a small degradation in accuracy and reliability – in comparison to real (observed) SSC residuals – one can use the transferred values of SSC for the calibration of outside geopotential models. We may add a small error to eq. (5) to roughly estimate precision of the linear transfer. This would lead to smaller values of r_t in eq. (7), however, so we do not apply this additional error source.

4.2. Single satellite crossovers JGM 3-based and GRIM5-S1 and C1 predicted

We recall Fig. 4 a,b,c,d with the SSC data (for ERS 1 and Geosat), JGM 3-based originals as well as the GRIM5-S1 transformed versions, plus Fig. 4 e,f with the formal *sd* of the data. For all these results the 4 day cut filter was used (later we show results with the shorter cut, 1.3 day). Note the *rms* of the data (around 10 cm) and their formal *sd* (around 1 cm), due to the long-term temporal averaging, and averaging of many measurements repeated over the same location (Sect. 2.3.). We have to rely upon these estimates. Nevertheless, it is interesting to test statistically whether or not this long-term averaged data may still be contaminated by additional systematic "non-gravitational" errors. These errors may originate from imperfect or neglected corrections in the altimetry data reduction process or from the failure of the cut-off filter to account properly for the 1 cpr orbit adjustments even in originally observed SSCs. This test is performed by means of the Student statistics (Sect. 2.5., eq. 7).

Before using the data from Fig. 4 or 6 for the calibration (for the ERS 2 case see Sect. 5.2), we show the results of the statistical treatment on Figs. 26a-c. We test the data $\delta\Delta X$ from Fig. 4 and 6 (we use their absolute values for the numerator of eq. 7), we use their sd from Fig. 4 e,f $s_{\delta\Delta X}$ (to the denominator of eq. 7), and the SSC errors from projections of the covariances s_{SSC} (again for the denominator of eq. 7). Note that s_{ng} is estimated to be about 1 cm, by experiments and experience. Note also that the observed or predicted SSC discrepancies are twice the error in $\Delta\delta$ propagated from the geopotential variance-covariances (eq. 1).

Figs. 26a-e provide a summary of the Student statistics for both satellites and all 3 gravity models. While with the JGM 3-based SSC, the ratio r_t is nearly everywhere below 1 and the null hypothesis is valid more or less everywhere (for more details see Klokočník et al., 1999), it is not the case for the new GRIM5-S1 and C1 SSC. There are belts with $r_t \geq 1$ mainly for ERS 1 and mainly in the central and south Pacific ocean. The test is especially rigorous for the more precise SSCs of ERS 1 (compare *rms* on Fig. 4c to *rms* on Fig. 4d). On the other hand, residual effects of poor altimetry corrections over the Pacific might contribute to these anomalies as well as unfiltered resonant perturbations with periods just below 4 days. However, with the 1.3 day cut, the Student statistics which were expected to support the null hypothesis better, did not. The reason is that the reduction of the resonant peaks in the predicted SSCs (in the numerator) is accompanied also by a lower SSC propagated error in the denominator of r_t.

As just mentioned the transfer from JGM 3 is responsible for the presence of certain resonant terms (14th and 15th order, and overtones) in the data on Fig. 4, for GRIM5-S1. Specifically this is due to the filter's cut for computations of the Q-functions in eq. 3. Many perturbations from shallow resonances have periods between 1 and 4 days. The shorter cut seems to simulate better the original filtering in JGM 3, which is nevertheless not known to us in detail. To be as fair

as possible with the statistics, we repeated the variance-covariance projections for ERS 1 and Geosat for JGM 3 and both new GRIMs with a cut of 1.3 days. We also repeated the statistics and present it in Figs. 26 d,e.

Fig. 26 c with the 1.3 day cut confirms the null hypothesis for both satellites (perfect for Geosat) when using the JGM 3 calibrated covariances (as shown by Klokočník et al, 1999, with the 4 day cut in that work; see also Fig. 26 a of this report).

For the GRIMs, the situation is more complicated. The dominant "along-track strips", being present in the SSC residuals of ERS 1, GRIM5-S1-predicted, accompanied with the 4 day cut (Fig. 26b), mostly dissapeared when the 1.3 day cut was applied (Fig. 26d). Thus, the null hypothesis may still apply for GRIM5-S1 but with doubts (mainly for Geosat, see the yellow-red "strips" in the Pacific area, Fig. 26 d, with $r_t \geq 1$).

For GRIM5-C1 and ERS 1 (Fig. 26 e), we already reject the null hypothesis because of the high number of locations with $r_t \geq 1$ and for their more or less systematic character.
Fortunately, this inconclusive situation has been clarified with the aid of ERS 2 SSC residuals (see Sect. 5.2).

5. Accuracy assessment with independent crossover altimetry

5.1. Accuracy assessment with altimetry from ERS 1 and Geosat

The SSC residuals JGM 3-based and GRIM5-S1-predicted for both ERS 1 and Geosat were used to calibrate these models in the sense of a check of the scaling factor of the formal variance-covariance matrix. (For JGM 3, we just outline the results from Klokočník et al, 1999). First, the SSC residuals are inverted to the LLC discrepancies (Sect. 2.4. and eq. 2), and then these are compared to the LLC errors projected for the respective satellite from the respective covariance matrices. Note again that we use the *rss* of LLC errors/discrepancies, computed from errors/discrepancies of both components C_m and S_m.

Figs. 27 and 29 show the adjusted LLC discrepancies from the given SSC residuals, with a 4 day cut for JGM 3 and 1.3 day cut for GRIM5-S1 and C1 (to suppress the filter problem coming from the linear transfer), to order 60, for ERS 1 and Geosat, respectively. Now, we compared these results with the LLC errors projected from variance-covariances, Figs. 17 and 18. In general, the observed (or predicted) discrepancies and their covariance-projected LLC errors over all latitudes and orders show a fair agreement in the magnitude of effects. Note that the z-axis on all these plots (Figs. 17, 18, 27, and 29) has the same scale.

A preliminary conclusion from this fast and raw comparison with the overall information on the 3D plots is that the variance-covariance matrices of JGM 3, GRIM5-S1 and GRIM5-C1 are almost correctly calibrated (or scaled). The agreement is evidently better for JGM 3 than for the GRIM5s. A detailed inspection is, however, necessary and this will disclose various inconsistencies that need to be explained.

To get a deeper insight, we computed mean and *rms* values of the powers of LLC errors or discrepancies over all latitudes and we present those for each order (Figs. 28 and 30 for ERS 1 and Geosat, Fig. 33b for ERS 1/ 2 data, see the next subsection). We also plot the powers of the

STR 00/22 German Research Centre for Geosciences
DOI: 10.2312/GFZ.b103-00228

LLC errors in detail for selected latitudes and lower and non-resonant orders separately (Fig. 31 a-d for ERS 1, e-f for ERS 1 and 2 SSC). The main resonant orders are excluded from futher testing due to possible problems with the orbit filter model for these orders (both in directly observed and predicted SSCs).

With regard to ERS 1 SSCs Figs. 28 and 30 show a very good agreement for JGM 3. Together with the Student statistics (Figs. 26 a,c) this confirms the correct calibration of the JGM 3 covariance matrix.

Figs. 28 and 30 indicate a still fair agreement for GRIM5-S1. However, for GRIM5-C1 and for ERS orbit, the agreement is not good enough, the scale factor of 5^2 seems to be too small. The problem is that the factor 5^2 fits well for Geosat. We cannot use different scale factors for different orbits. A possible explanation is that for GRIM5-C1 and ERS, our testing data (the SSC residuals) are themselves not accurate enough and/or that they contain too large residual "non-gravitational" errors. This is well possible – see the Student statistics – noting the very small amplitude of the power of LLC discrepancies for ERS 1 with GRIM5-C1. For the tests with ERS 2 data, see the next subsection.

Figs. 31a-d is one of many examples we have for the individual orders of harmonics, where we compare the observed and predicted LLC discrepancies/errors. Here we show four gravity models for the ERS-type orbit with the ERS 1 SSCs, "observed" with JGM 3, and "predicted" for EGM 96, GRIM5-S1 and C1. The best for m=1–3 is the GRIM5-C1 and S1, which probably means their lower contamination by non-static gravity field signals. We already had some objections against m=1 and 3 in the case of JGM 3 in our previous analysis (Klokočník et al, 1999).

5.2. Accuracy assessment with ERS 1 and ERS 2 altimetry

Figs. 27–30 and 28c reveal a correct calibration only for JGM 3 (both ERS 1 and Geosat) and in the case of the new GRIMs only for Geosat. For GRIM5-S1 and particularly C1, our ERS 1 SSC residuals, although precise and independent, were not accurate enough to decide on the correctness of the scale factor (5^2) for the new models. Recently, however, we have gathered almost 2 million crossovers from a combination of ERS 1 and ERS 2 altimetry and these have helped to resolve this problem. The results concerning the contribution of ERS 2 SSC to the calibration are shown on Figs. 32 a-e (crossover residuals), Fig. 32 f and Figs 33 a,b (statistics), Fig. 33 c (powers of LLC discrepancies), Fig. 33 d (the main comparison between the "observations" and projections), and Figs. 31 e-f (LLC errors for the individual orders).

The new data come from the NASA Pathfinder altimetry data sets (Koblinsky et al, 1999). They cover 47 cycles (with the 35 day repeat period) in the interval 1995 – 1999 (while ERS 1 covers only 18 such cycles in 1992–1993). These 47 first cycles of ERS 2 were combined with the first 18 cycles of ERS 1 in 2x3 deg bin (latitude *vs* longitude) averaging over 1.800000 SSC residuals.

The ERS 1 and 2 crossovers were originally DGM-E04 based (Figs. 32 a-c), and thus they were linearly transformed from that model to yield predicted observations for GRIM5-C1 (Figs. 32 e-f), using a 1.3 day cut of terms. In comparison with ERS 1 altimetry, the new data are considerably more precise (compare Figs. 32 a-e to Figs. 6a and 4e). This fact in particular can be deduced from Fig. 32f.

STR 00/22 German Research Centre for Geosciences
DOI: 10.2312/GFZ.b103-00228

The orbit of ERS 2 is more precisely known to begin with, thanks to microwave PRARE tracking in addition to laser tracking, and also the altimetry correction scheme should be more objective in some details. For the sea state bias in ERS 1 altimetry, Koblinsky et al (ibid) used only a simple 5.5% of the significant wave height which they thought was not sufficient. In ERS 2, they used a Gaspar 3 parameter model including wind speed. For ionospheric correction, Koblinsky et al (ibid) used the IRI 95 model for both satellites. But we note that ERS 1 was closer to a solar maximum than most of the ERS 2 mission and so whatever model was used for ionosphere is likely to have introduced larger errors for ERS 1 than for ERS 2 altimeter. On Fig. 32 c, we display the difference ERS 1–ERS 2 SSC and we see a significant difference – a broad feature in the Pacific and a large difference in the northern Indian ocean. It is due to altimetry corrections problem but it is difficult to say of which satellite, probably both.

The Student statistics with the ERS 1/ 2 SSC combination (Fig. 33 b) was a surprise. When compared to the statistics with the ERS 1 SSC alone (Fig. 26e or 33a), it looks similar. So one might be inclined to assume too small variance-covariance scaling factor again. While the variance-covariance projection from GRIM5-C1 to the crossover error s_{SSC} is the same in both cases (like Fig. 9, but smaller here with a 1.3 day cut), the data error $s_{\delta\Delta X}$ is much smaller with ERS 2 (compare Fig. 4e and 32e,f). The SSC residuals ERS 1/2 are also smaller and therefore, the statistics give similar answers.

We continue with the transform of the ERS 1 and 2 crossovers (DGM-E04 based) to the LLC discrepancies (the 3D plot, Fig. 33c) and – as before – we compare the *rms* power of the LLC errors and discrepancies (Fig. 33d). The power of LLC discrepancies on Fig. 33c should be compared with that on Fig. 27c. We do see a much smaller LLC signal with the new data (as was expected from Fig. 32d).

Indeed, compared to Fig. 28c, Fig. 33d presents now a very good agreement of the *rms* of powers of the LLC discrepanies and errors. *We have verified with the aid of ERS 2 SSC residuals the scaling factor 5^2 for the formal variance-covariance matrix of GRIM5-C1.*

Note that to account for the effect in analogy to s_{ng} in eq. 5 for the *rms* power of LLC discrepancies/errors on Figs. 28, 30, 33c, we had to add about 1 mm or 0.5 mm to the green curves for ERS 1 or 2 for each order. This was an estimate for the contribution of the "non-gravitational" effects transformed from the crossovers to the LLC errors, and distributed evenly for all orders. This small correction helps to improve the comparison.

Figs. 31e-f is one of many examples we have for the individual orders of harmonics, where we compare the observed and predicted LLC errors/discrepancies for the ERS 1/2 combined SSC residuals based upon 3 gravity models which have used ERS-type orbits in their development (JGM 3, GRIM5-C1 and DGM-E04). The predictions from the covariances here shown (in black dashed lines) are the same as on Fig. 17a-d (for a few low orders separately). We realize an evident progress from JGM 3 to GRIM5-C1 and a fair agreement between the "observed" LLC discrepacies with GRIM5-C1 (green data with formal *sd*) and the projected LLC errors from GRIM5-C1 variance-covariances (black dashed curves). Note the fine scale in centimeters.

6. Conclusions and outlook

The new GFZ and GRGS gravity field models GRIM5-S1 and GRIM5-C1 were compared with other recent models by means of projections of the scaled covariance matrix of their harmonic geopotential coefficients to radial orbit errors (and its components) in geographical representation and to the latitude lumped coefficient errors. The comparison shows an excellent performance of GRIM5-C1 for ERS 1/2, TOPEX/Poseidon, and GFZ 1 orbits, as the data from these satellites are well represented in the gravity models. For the Geosat type orbit, JGM 3 and EGM 96 perform better than GRIM5-C1 or S1. For CHAMP, all models are roughly of the same quality. The radial error at the inclination of CHAMP has strongly zonal character. The satellite-only solution GRIM5-S1 cannot of course compete with the combined solutions (GRIM5-C1, EGM 96, JGM 3), but it performs very well again for ERS, T/P, and GFZ 1.

The latitude lumped coefficients (LLC) are discriminating the error contributions order by order to the total radial error and thus provide a better insight into the accuracy distribution. We use them for comparisons too, and confirmed the results obtained by the full geographical representation of the radial error. It is often the case that errors in only a few orders of harmonic coefficients dominate the whole radial error. These are the shallow resonant orders (and their overtones) and a few lowest orders. These orders could be further improved (with the incorporation of crossover altimetry) in geopotential model development. The LLC presentation shows that in some cases the traditional orbit tests are not sufficient to objectively describe the orbit error in detail.

While improvements in gravity field modelling during the last decade has been considerable, the models are still internally inhomogenous from the viewpoint of radial errors. With a high dependence on the orbit inclination, models provide a widely varying radial accuracy. The largest errors are logically for the low inclined orbits (with poor tracking records), but a local maximum of the radial error also occurs for nearly-polar prograde orbits. This is true for satellite-only models as well as for the combined models (with surface information also), older as well as the most recent models. We see that there is still a large opening for further improvements.

Long-term averaged single satellite crossover (SSC) residuals of ERS 1 and Geosat, completely independent of GRIM5-S1 and C1 models, were linearly transferred to yield GRIM5-S1 and GRIM5-C1–predicted values. These SSC discrepancies were then adjusted into LLC values after binning the SSCs into latitudinal bands. Finally, the predicted LLC were compared to the relevant LLC errors projected from the calibrated/scaled variance-covariances of JGM 3, GRIM5-S1 and GRIM5-C1.

Note that the SSC residuals and their formal errors also passed Student statistical test to detect possible residual errors of "non-gravitational" origin. These errors are present and contaminate the SSC residuals, namely for ERS 1 and the GRIM5 models.

Based on SSC residuals of ERS 1 and Geosat, we confirmed our previous result (Klokočník et al, 1999) that the JGM 3 covariance matrix is well calibrated (not too optimistic, but excluding orders 1 and 3 for ERS 1). For GRIM5-S1 the scale factor of its variance-covariance matrix is still acceptable, but for the most precise model of our "tested file", GRIM5-C1, the factor should be higher in the case of ERS type orbits. The scale factor, however, must be the same for all orbits in the frame of one gravity model. The factor fitting for ERS 1 would be too pessimistic for Geosat. A preliminary conclusion was that while for JGM 3 (and GRIM5-S1) our testing data base (the SSC residuals after full corrections) is sufficiently accurate, for GRIM5-C1 and ERS 1 it is not.

With the aid of ERS 2 SSC, combined with our ERS 1 data, we achieved a much stronger calibrational tool and we have verified in an unique way also GRIM5-C1 covariance scaling for ERS-type orbits. In summary, the scaling factor 5^2 is confirmed as a good overall choice to scale the formal variance-covariance matrix of the GRIM5-C1 solution.

Gravity field evaluation becomes more and more difficult as the residual non-gravitational effects are now at the same level or larger than the gravitational modelling errors.

Gravity field model evaluation by means of single-satellite altimetry crossovers, independent of the tested models, is one of many tests which can be performed to know better the quality and performance of these models. The tests presented here for the pre-CHAMP gravity models GRIM5-S1 and C1 will be repeated with a gravity field model incorporating CHAMP data, for a comparison and to assess the actual contribution of the CHAMP data. While the SSC data provided a sensitive check for the pre-CHAMP models, it is likely that the CHAMP data due to their high accuracy may provide a good check of the SSC data (e.g., for non-gravitational error sources in the altimetry).

It is recommended to compute "true" SSC and DSC residuals between and among ERS 1, 2, Geosat or GFO and T/P or Jason, over long intervals (multi-year sets), based on a forthcoming gravity model from CHAMP. Finally, if referred to the initial model of a gravity field solution, these data can be added into one of the next adjustments for the gravity field parameters.

A study of resonant phenomena in the decaying orbit of CHAMP can provide accurate values of the traditional (dynamic) lumped coefficients for specific orders which can test and possibly also improve certain resonant terms in the comprehensive solutions for the geopotential.

Acknowledgements

Study was performed when lead author worked as guest scientist at GFZ, Potsdam. Support from GFZ is greatly appreciated. This investigation has partly been done also in the frame of grant of GA AV of the Czech Republic A3004 and supported by the project LN00A005 by the Ministry of Education of the Czech Republic. We thank John Lillibridge for supplying the NOAA SSCs on ERS 1 used to test the transfer algorithm.

References

Biancale R, Balmino G, Lemoine J M, Marty J C, Moynot B, Barlier F, Exertier P, Laurain O, Gegout P, Schwintzer P, Reigber CH, Bode A, Koenig R, Massmann F H, Raimondo J C, Schmidt R, Zhu SY 2000: A New Global Earth's Gravity Field Model from Satellite Orbit Perturbations: GRIM5-S1, subm. to *Geophys. Res. Letts.*.

Gruber T, Bode A, Reigber Ch, Schwintzer P, Balmino G, Biancale R, Lemoine J M, 2000: GRIM5-C1: Combination Solution of the Global Gravity Field to Degree and Order 120, subm. to *Geophys. Res. Letts.*.

Klokočník J, Kobrle F 1992: Dual-Satellite Crossover Altimetry for ERS-1/TOPEX, *Adv. Space Res.* **13**, (11) 335-337.

Klokočník J, Wagner C A, Kobrle F 1992: A Test of GEM T2 from GEOSAT Crossovers using Latitude Lumped Coefficients, *Proceedings IAG Symp. 112*, eds. H.Montag and Ch. Reigber, Springer Verlag, pp.79–82.

STR 00/22 German Research Centre for Geosciences
DOI: 10.2312/GFZ.b103-00228

Klokočník J, Lemoine F G, Kostelecký J 1998: Reduction of Crossover Errors in the Earth Gravity Model (EGM 96), *Marine Geod.*, **21**, 219–239.

Klokočník J, Wagner C A (1999), Combinations of Satellite Crossovers to Study Orbit and Residual Errors in Altimetry, *Celest. Mech. and Dynam. Astr.* **74**, 231–242.

Klokočník J, Wagner C A, Kostelecký J, Jandová M 1995a: Altimetry with Dual-Satellite Crossovers, *Manuscr. Geod.*, **20**, 82–95.

Klokočník J, Wagner C A, Kostelecký J, Jandová M 1995b: The Filtering Effect of Orbit Correction on Geopotential Errors, *J. Geod.*, **70**, 146–157.

Klokočník J, Wagner C A, Kostelecký J 1996: Accuracy Assessment of Recent Earth Gravity Models Using Crossover Altimetry, *Studia geoph. et geod.*, **40**, 77–110.

Klokočník J, Wagner C A, Kostelecký J 1999: Spectral Accuracy of JGM 3 from Satellite Crossover Altimetry, *J. Geod.*, **73**, 138–146.

Klokočník J, Wagner C A, Kostelecký J 2000: Residual Errors in Altimetry Data Detected by Combinations of Single- and Dual-Satellite Crossovers, *J. Geod.*, **73**, 671–683.

Koblinsky C J, Ray R, Beckley B, Wang Y M, Tsaoussi L, Brenner A, Williamson R 1999: *NASA Ocean Altimeter Pathfinder Project*, Rep. 1: Data Processing Handbook, NASA/TM-1998-208605.

Lemoine FJ, Kenyon SC, Factor JK, Trimmer RG, Pavlis NK, Chinn DS, Cox CM, Klosko SM, Luthcke SB, Torrence MH, Wang ZM, Williamson RG, Pavlis EC, Rapp RH, Olson TR 1998: *The Development of the Joint NASA GSFC and the National Imagery and Mapping Agency (NIMA) Geopotential Model EGM 96*, NASA/TP-1998-206861.

Reigber Ch, Lűhr H, Schwintzer P 2000: CHAMP mission status, subm. to *Adv. Space Res.*.

Rosborough G W 1986: *Satellite Orbit Perturbations due to the Geopotential*, CSR-86-1 Univ. of Texas at Austin, Center for Space Research.

Scharoo R, Visser P 1998: Precise Orbit Determination and Gravity Field Improvement for the ERS Satellites, *J. Geophys. Res.* **103** (C4), 8113–8127

Schwintzer P, Reigber Ch, Bode A, Kang Z, Zhu SY, Massmann FH, Raimondo JC, Biancale R, Balmino G, Lemoine JM, Moynot B, Marty JC, Barlier F, Boudon Y 1997: Long-wavelength Global Gravity Field Models: GRIM 4 S4, GRIM 4 C4, *J. Geod. 71*, 189–208.

Tapley BD, Watkins MM, Ries JC, Davis GW, Eanes RJ, Poole SR, Rim HJ, Schutz BE, Shum CK, Nerem RS, Lerch FJ, Marshall JA, Klosko SM, Pavlis NK, Williamson RG 1996: The Joint Gravity Model 3, *J. Geophys. Res.*, **101** (B12), 28029–28049.

Wagner C A 1989: Summer School Lectures on Satellite Altimetry, *Lect. Notes Earth Sci. 25*, Theory of Satellite Geodesy and Gravity Field Determination, Ed. F. Sansó and R. Rummel, pp. 285–334, Springer-Verlag, New York.

Wagner C A, Klokočník J 1994: Accuracy of the GEM T2 Geopotential from GEOSAT and ERS-1 Crossover Altimetry, *J. Geophys. Res.* **99**, B5, 9179–9201.

Wagner C A, Klokočník J, Tai C K, 1995: Evaluation of JGM 2 Geopotential Errors from Geosat, TOPEX/Poseidon and ERS-1 Crossover Altimetry, *Adv. Space Res.*, **16**, (12) 131–141.

Wagner C A, Klokočník J, Cheney R E 1997a: Making the Connection between Geosat and TOPEX/Poseidon, *J. Geod.* **71**, 273–281.

Wagner C A, Klokočník J, Kostelecký J 1997b: Dual-Satellite Crossover Latitude-Lumped Coefficients, their use in Geodesy and Oceanography, *J. Geod.* **71**, 603–616.

Wagner C A, Klokočník J, Kostelecký J 2000: Geopotential and Oceanographic Signals from Inversion of Single and Dual satellite Altimetry, VUGTK technical report **46**, no. 26., see also web pages: *http://ibis.grdl.noaa.gov/ SAT/pubs/papers/wagner_2000* or *http://panurgos.fsv.cvut.cz/~ kost/eur00.html*

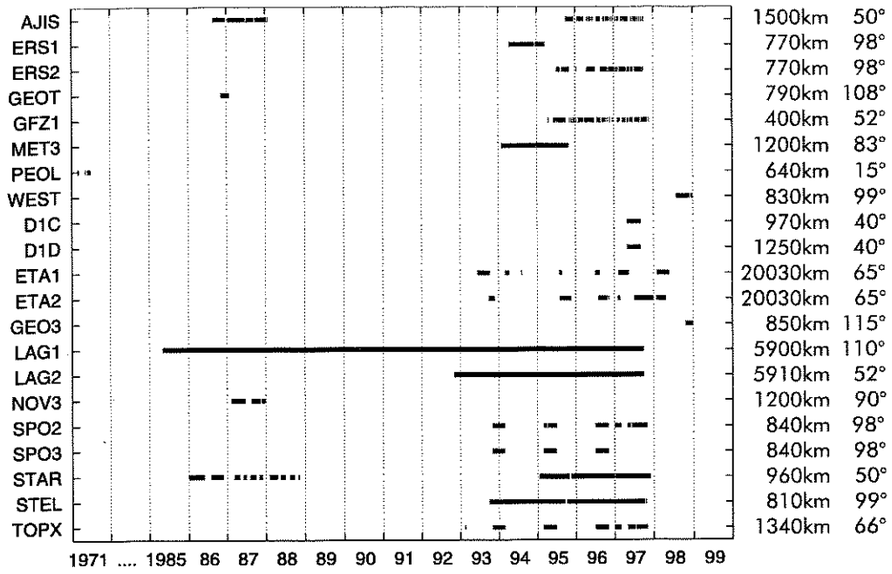

Fig. 1. Satellite data base for GRIM5-S1 and C1 models. From Biancale et al. (2000).

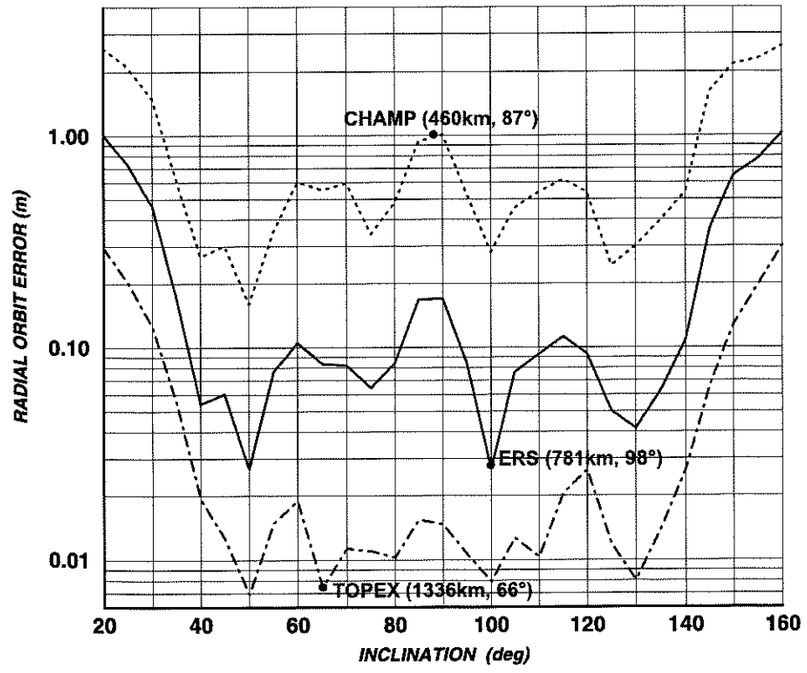

Fig. 2. Expected radial orbit error as a function of orbit inclination and altitude, due to the scaled covariances of the GRIM5-S1 harmonic geopotential coefficients (Biancale et al. 2000). The three altitudes corresponds to CHAMP, ERS and T/P orbits, respectively.

STR 00/22 German Research Centre for Geosciences
DOI: 10.2312/GFZ.b103-00228

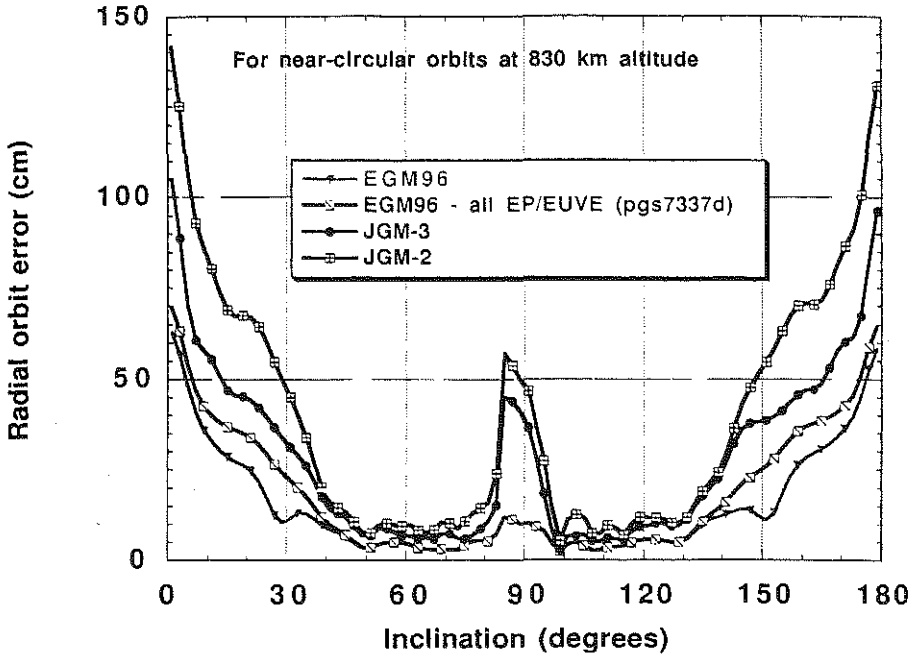

Fig. 3. Expected radial orbit error as a function of orbit inclination, due to the scaled covariances of the harmonic geopotential coefficients. The case of several gravity field models (from JGM 2 to EGM 96) for selected height (830 km) to show evolution and increasing quality of the models. From Lemoine et al (1998), p.:10-40.

DOI: 10.2312/GFZ.b103-00228

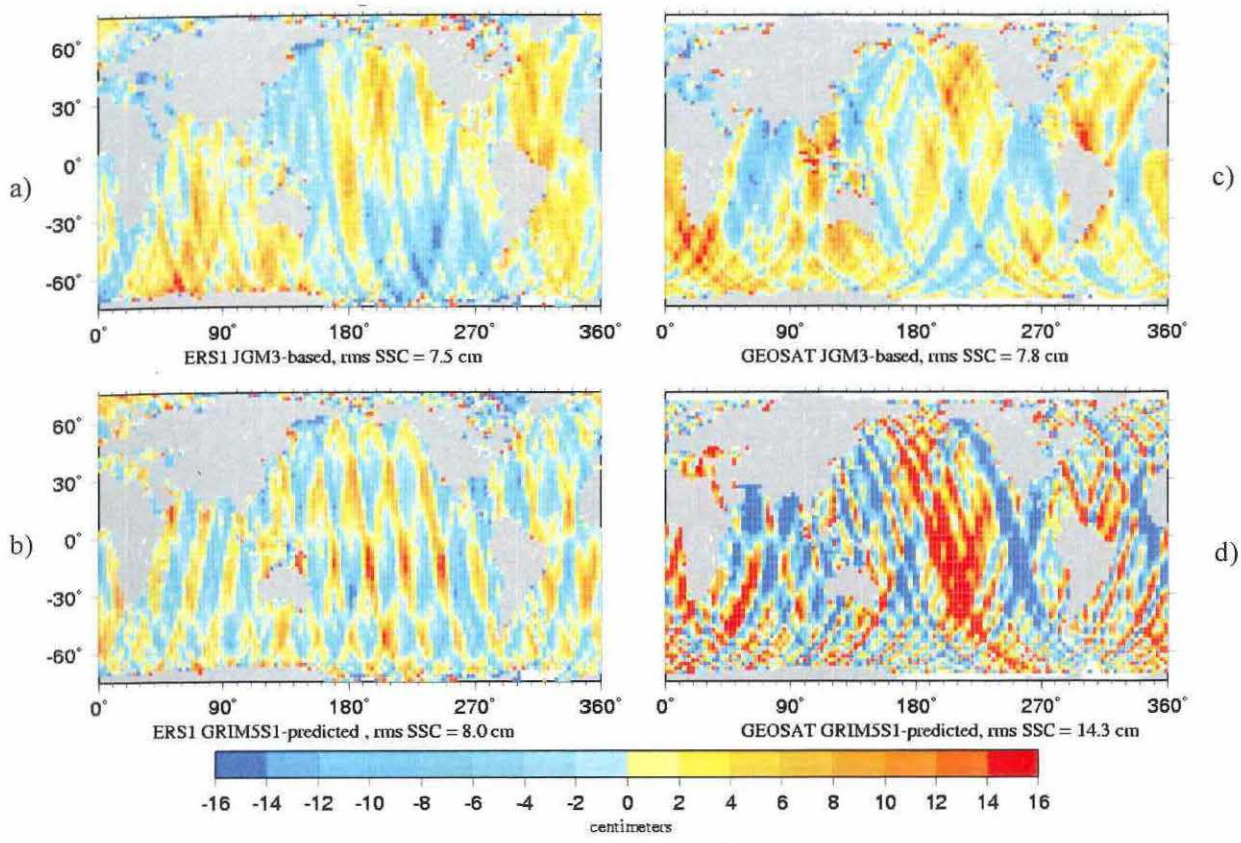

Fig. 4 a,b,c,d: The data set: corrected SSC residuals for ERS1 and Geosat with Jgm3 and GRIM5S1. Always with 4 day cut of orbit perturbations.

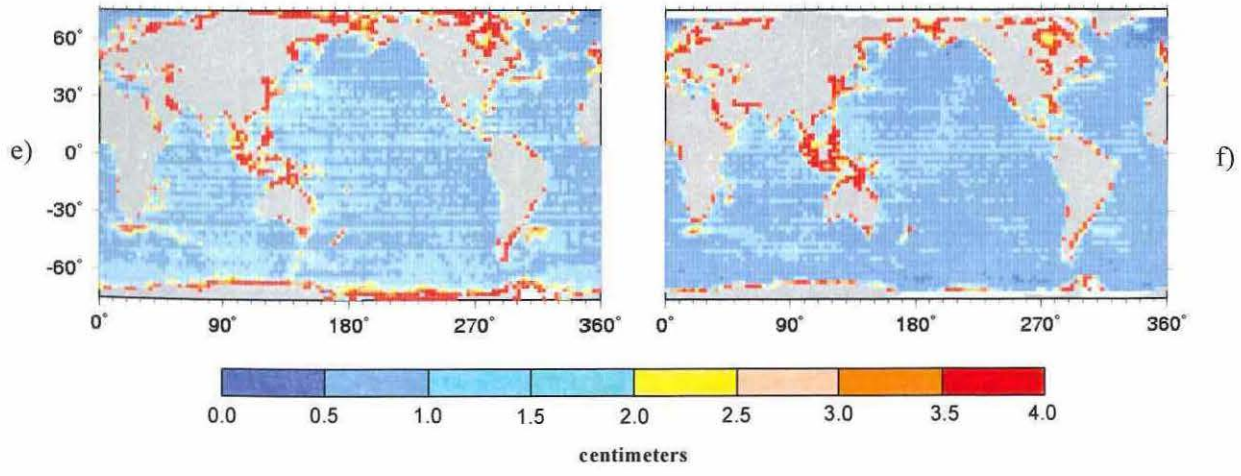

Fig. 4 e,f.: Formal standard deviations of the corrected SSC residuals for ERS1 and Geosat, Jgm3-based. Note the scale different from scale on Figs. 4 a-d.

DOI: 10.2312/GFZ.b103-00228

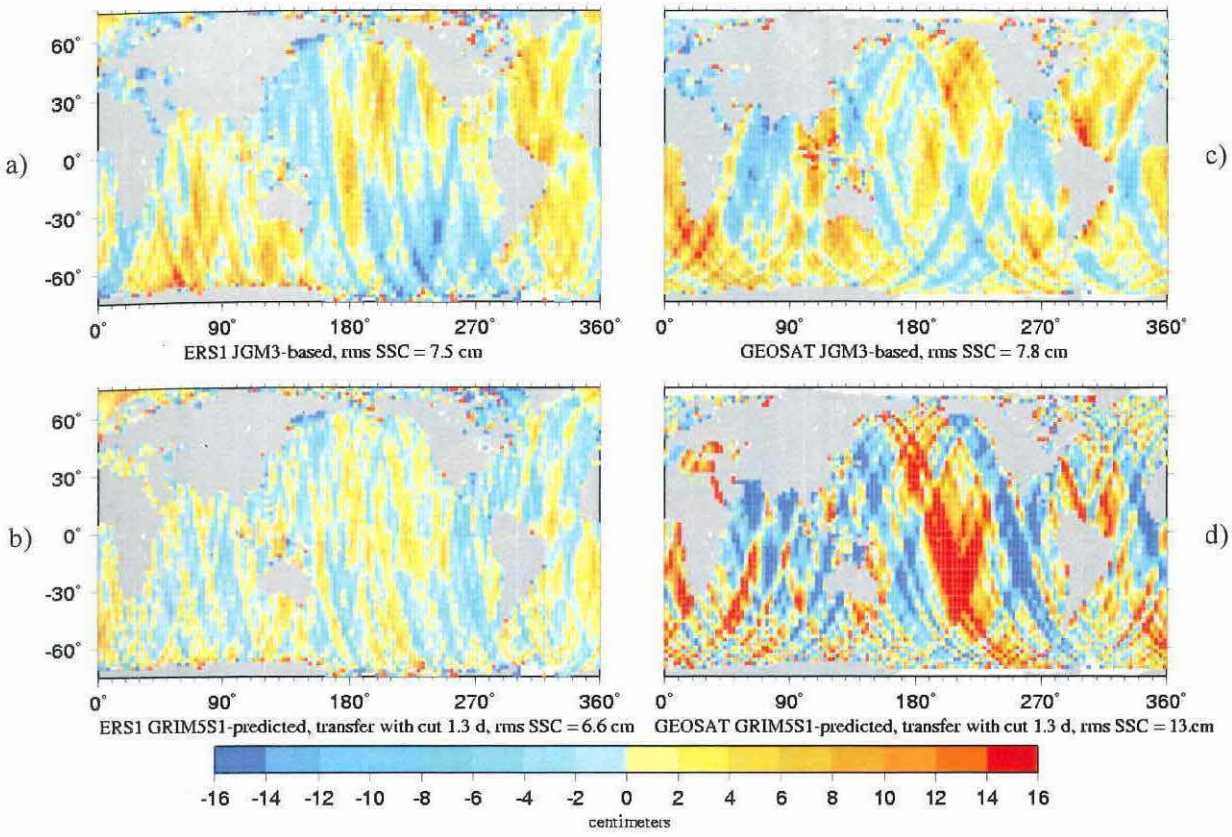

Fig. 5.: The data set: corrected SSC residuals
for ERS1 and Geosat with JGM3 and GRIM5S1- predicted.
Always with 1.3 day cut of orbit perturbations.

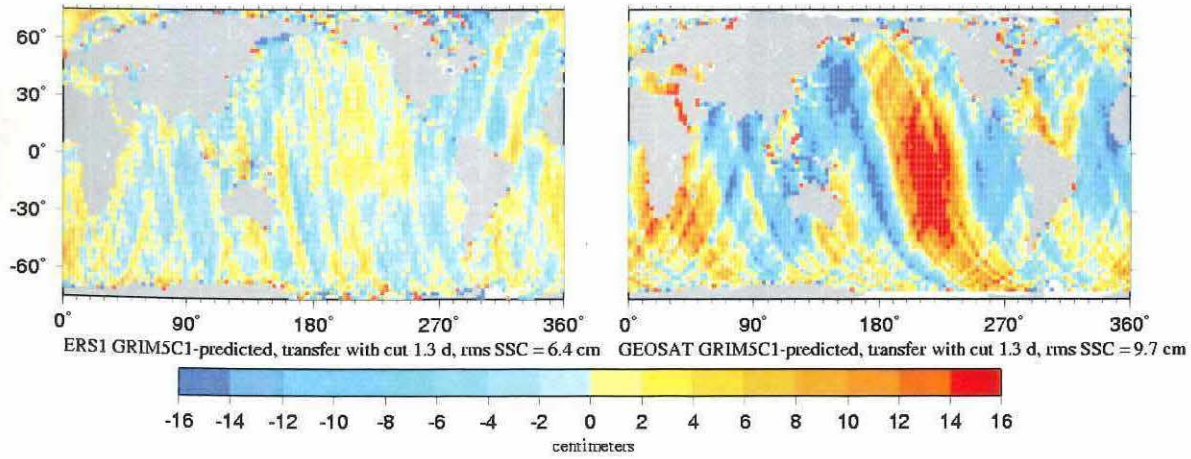

Fig. 6.: The data set: corrected SSC residuals
for ERS1 and Geosat GRIM5C1- predicted.
The 1.3 day cut of orbit perturbations used for
the original as well as predicted SSC.

DOI: 10.2312/GFZ.b103-00228

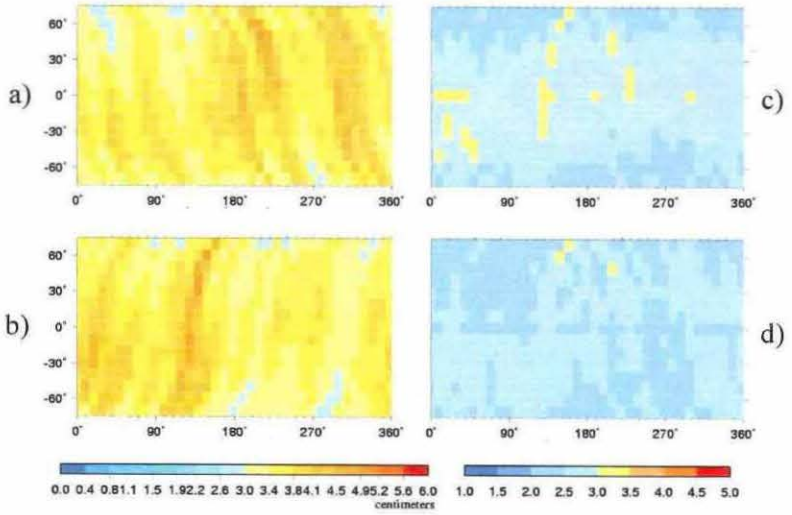

Fig. 7.: Radial error for ERS 1 with Jgm3 covariances, 4 day cut:
(a) radial error in ascending track, rms = 3.7 cm,
(b) radial error in descending track, rms = 3.6 cm,
(c) geographically correlated (mean) part of the radial error, rms = 2.6 cm,
(d) anti-correlated (variable) part of the radial error, rms = 2.5 cm.

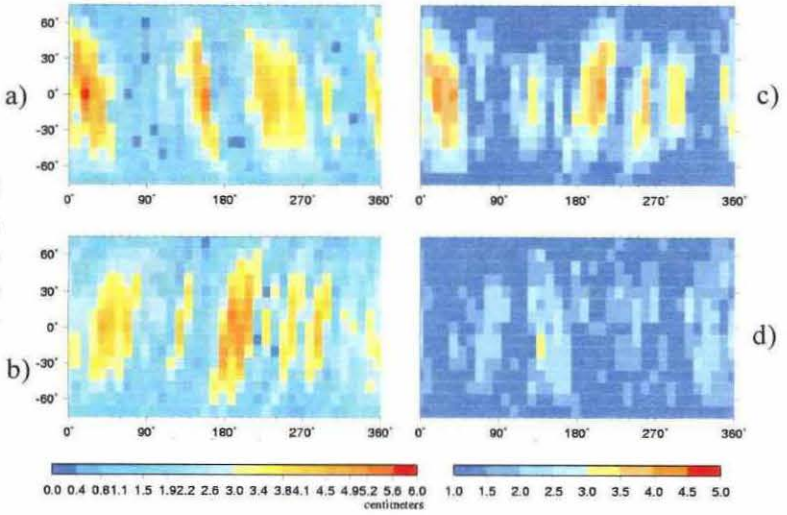

Fig. 8.: Radial error for ERS 1 with GRIM5S1 covariances, 4 day cut:
(a) radial error in ascending track, rms = 2.4 cm,
(b) radial error in descending track, rms = 2.5 cm,
(c) geographically correlated (mean) part of the radial error, rms = 2.0 cm,
(d) anti-correlated (variable) part of the radial error, rms = 1.5 cm.

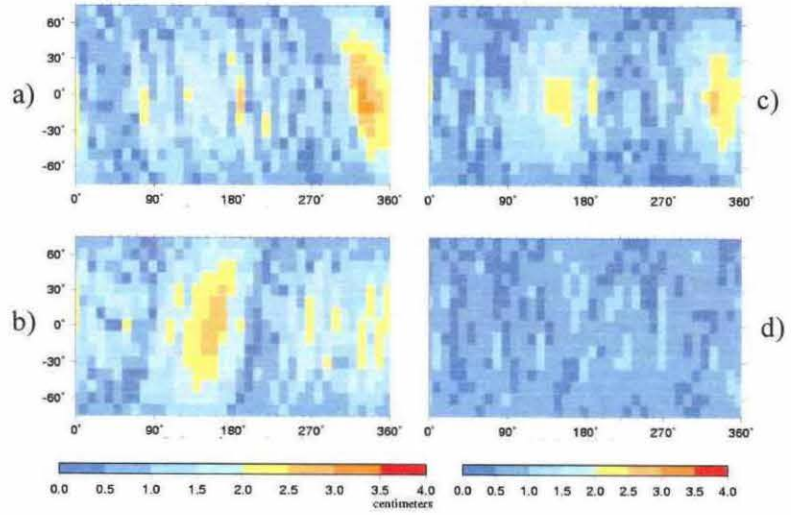

Fig. 9.: Radial error for ERS 1 with GRIM5C1 covariances, 4 day cut:
(a) radial error in ascending track, rms = 1.2 cm,
(b) radial error in descending track, rms = 1.2 cm,
(c) geographically correlated (mean) part of the radial error, rms = 0.9 cm,
(d) anti-correlated (variable) part of the radial error, rms = 0.5 cm.

DOI: 10.2312/GFZ.b103-00228

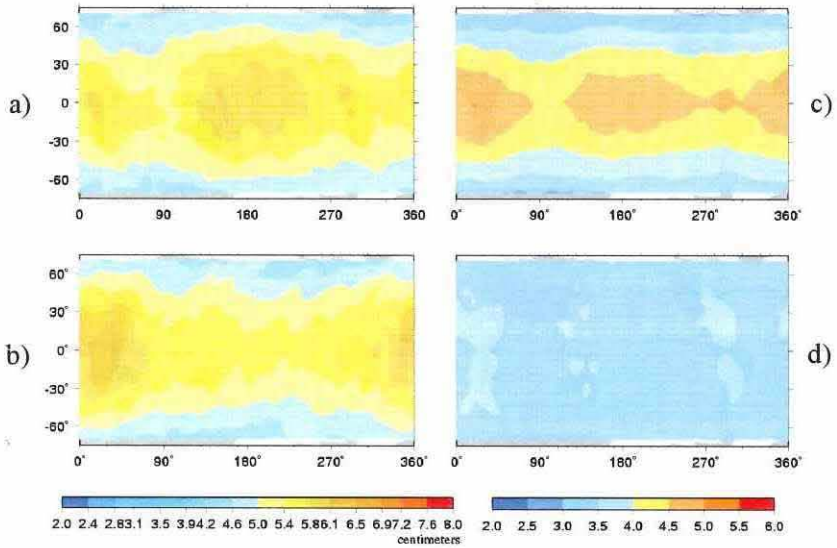

Fig. 10.: Radial error for Geosat with Jgm3 covariances, 4 day cut:
(a) radial error in ascending track, rms = 5.1 cm,
(b) radial error in descending track, rms = 5.0 cm,
(c) geographically correlated (mean) part of the radial error, rms = 4.2 cm,
(d) anti-correlated (variable) part of the radial error, rms = 3.5 cm.

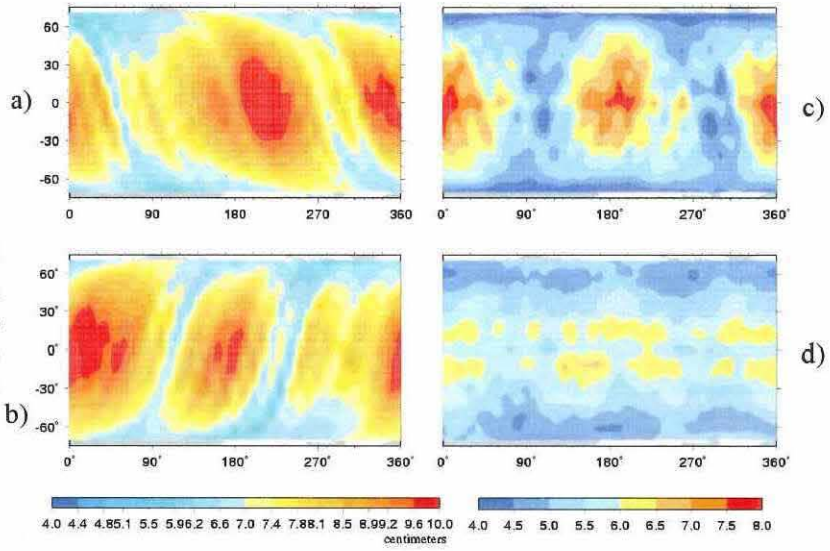

Fig. 11.: Radial error for Geosat with GRIM5S1 covariances, 4 day cut:
(a) radial error in ascending track, rms = 7.4 cm,
(b) radial error in descending track, rms = 7.3 cm,
(c) geographically correlated (mean) part of the radial error, rms = 5.1 cm,
(d) anti-correlated (variable) part of the radial error, rms = 4.9 cm.

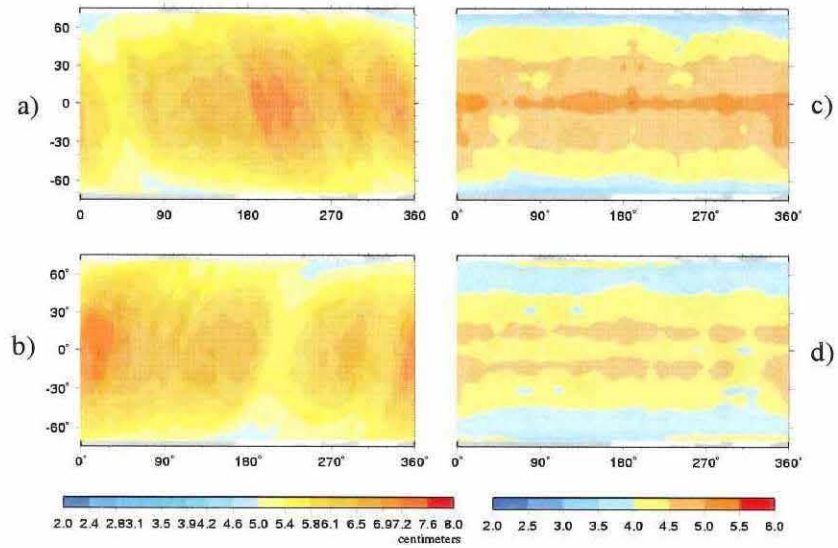

Fig. 12.: Radial error for Geosat with GRIM5C1 covariances, 4 day cut:
(a) radial error in ascending track, rms = 5.6 cm,
(b) radial error in descending track, rms = 5.6 cm,
(c) geographically correlated (mean) part of the radial error, rms = 3.9 cm,
(d) anti-correlated (variable) part of the radial error, rms = 3.7 cm.

DOI: 10.2312/GFZ.b103-00228

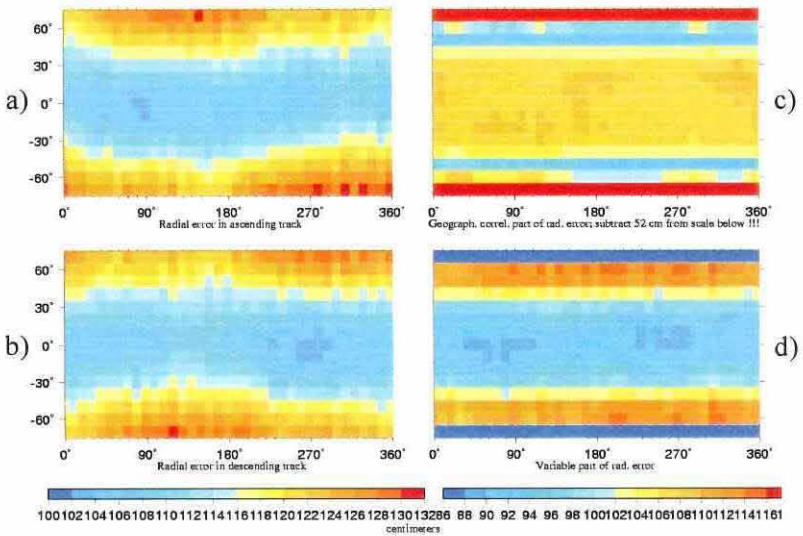

Fig. 13.: Radial error for CHAMP with Jgm3 covariances, 4 day cut:
(a) radial error in ascending track, rms = 117 cm,
(b) radial error in descending track, rms = 117 cm,
(c) geographically correlated (mean) part of the radial error, rms = 66 cm,
(d) anti-correlated (variable) part of the radial error, rms = 96 cm.

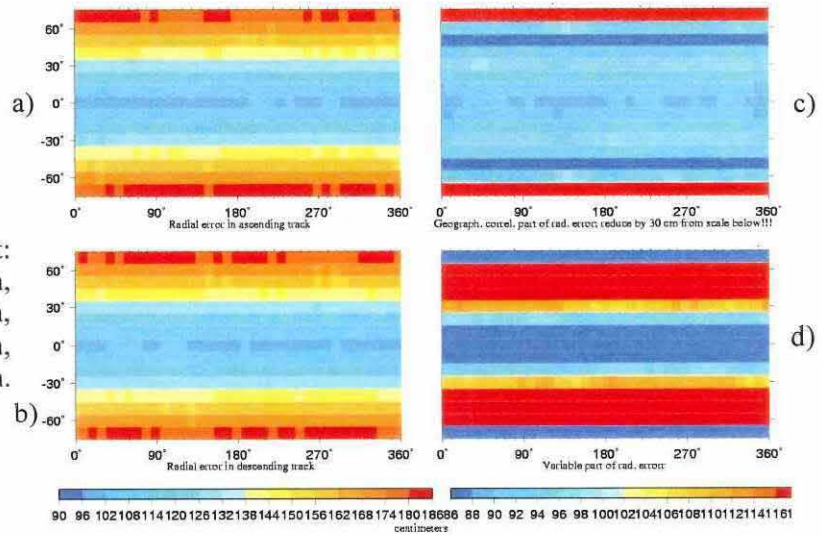

Fig. 14.: Radial error for CHAMP with GRIM5S1 covariances, 4 day cut:
(a) radial error in ascending track, rms = 149 cm,
(b) radial error in descending track, rms = 149 cm,
(c) geographically correlated (mean) part of the radial error, rms = 91 cm,
(d) anti-correlated (variable) part of the radial error, rms = 117 cm.

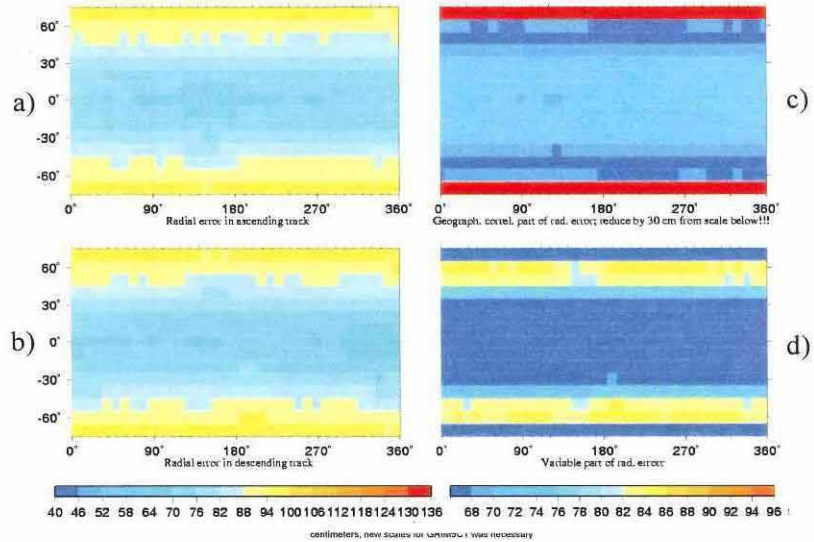

Fig. 15.: Radial error for CHAMP with GRIM5C1 covariances, 4 day cut:
(a) radial error in ascending track, rms = 85 cm,
(b) radial error in descending track, rms = 85 cm,
(c) geographically correlated (mean) part of the radial error, rms = 52 cm,
(d) anti-correlated (variable) part of the radial error, rms = 67 cm.

DOI: 10.2312/GFZ.b103-00228

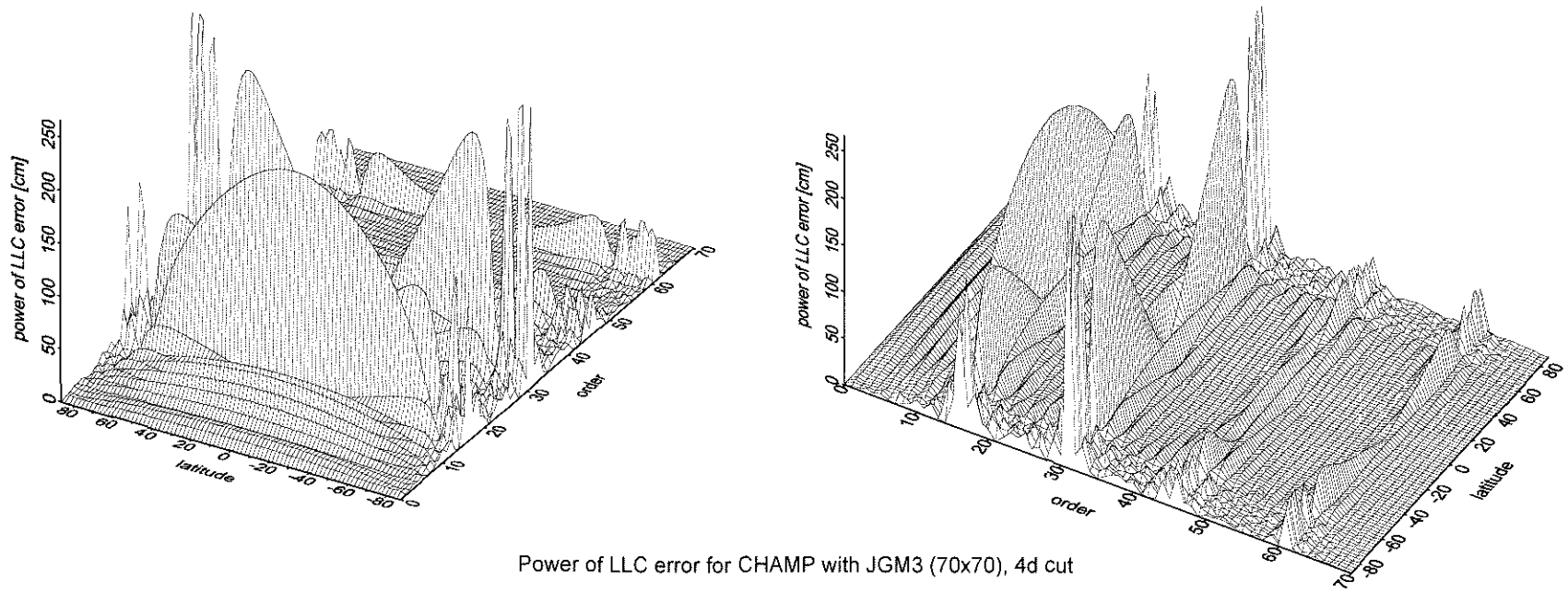

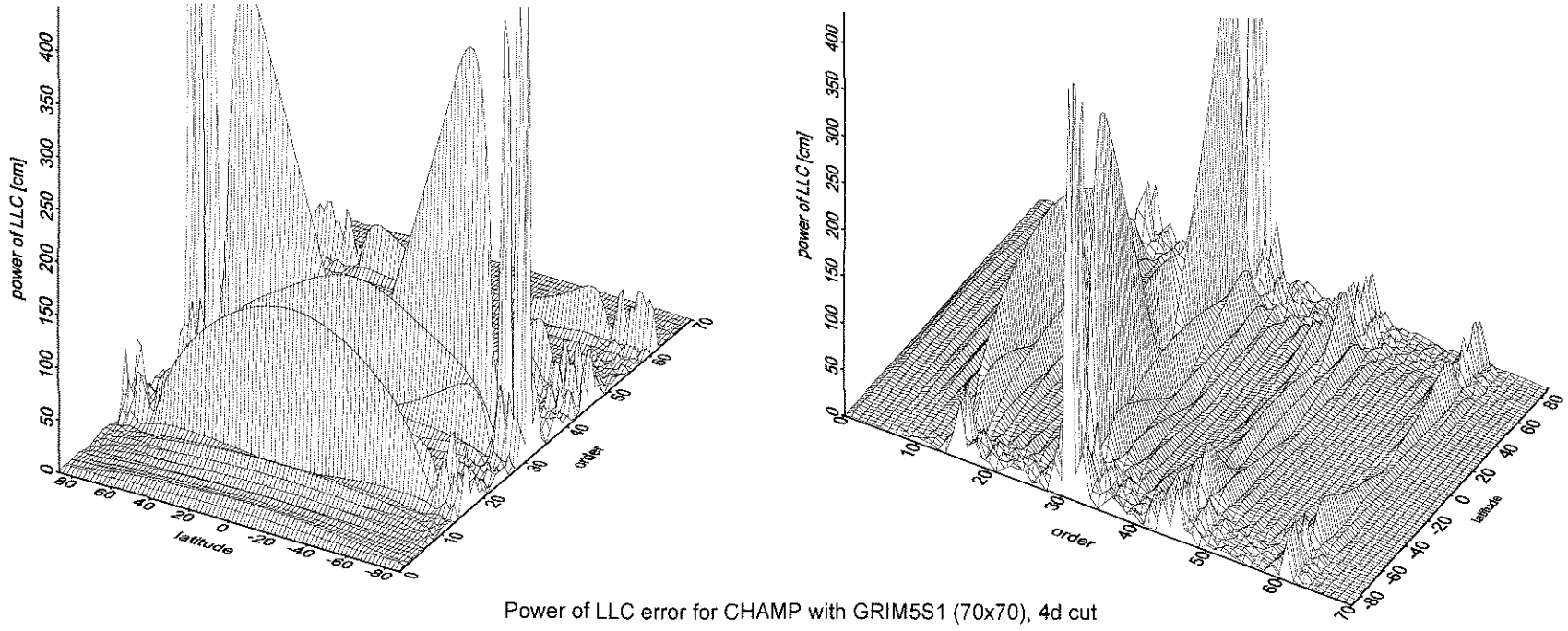

Fig. 16.: A first look on the error of latitude lumped coefficients: an example for CHAMP with the Jgm3 and GRIM5S1 covariances, and the 4 day cut of orbit perturbations. Note scale. The LLC errors for some orders are hidden behind the others (left hand side); thus, we added plots after a rotation (right hand side)

STR 00/22 German Research Centre for Geosciences
DOI: 10.2312/GFZ.b103-00228

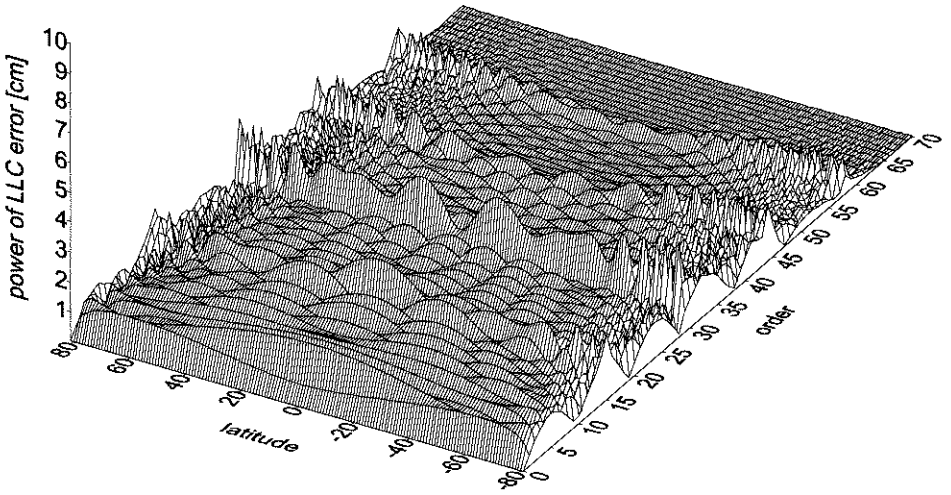

Power of LLC errors for ERS1 with JGM3 (70x70), 4d cut

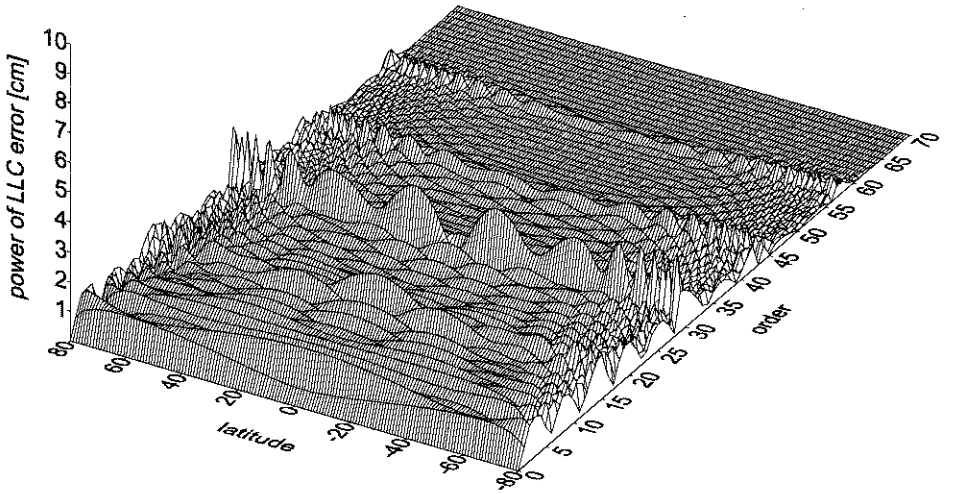

Power of LLC error for ERS1 with EGM96 (70x70), 4 d cut

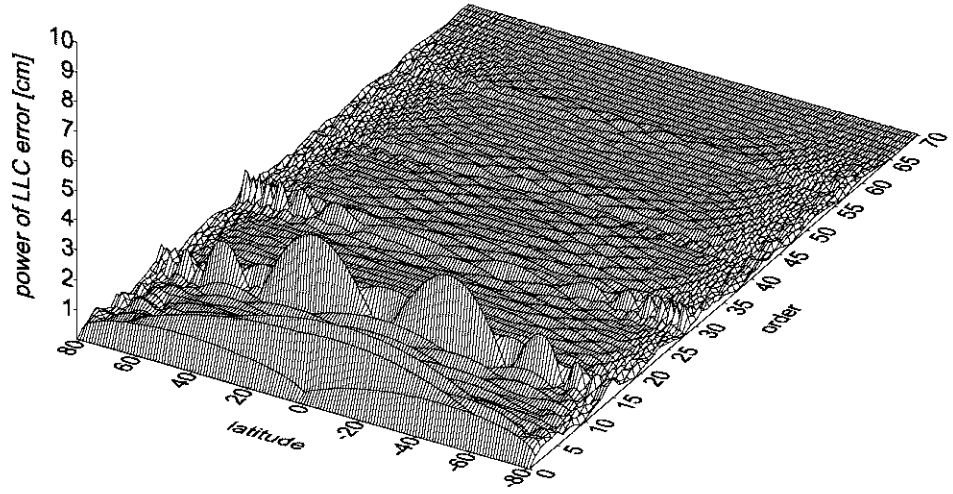

Power of LLC error for ERS 1 with GRIM5S1 (70x70), 4 d cut

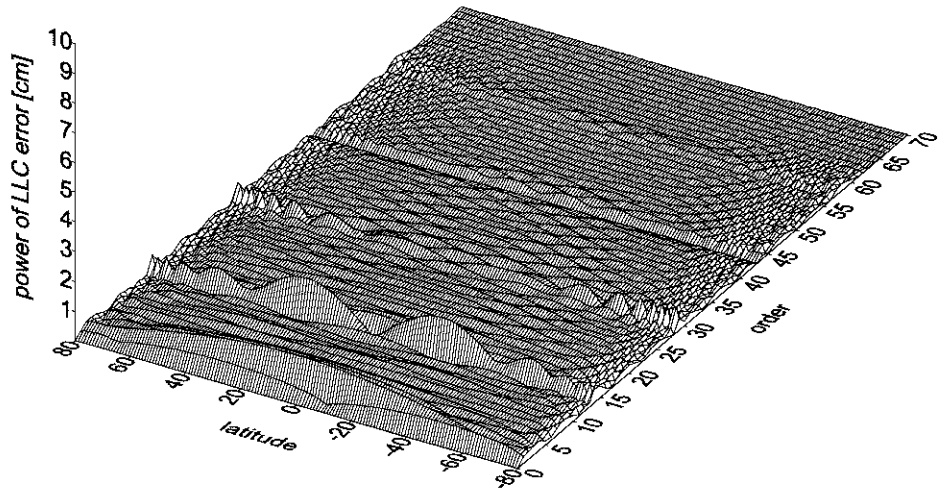

Power of LLC error for ERS 1 with GRIM5C1 covar (70x70), 4 d cut

Fig. 17.: Error of latitude lumped coefficients for ERS 1 with Jgm 3, EGM 96, GRIM5S1 and GRIM5C1 covariances, 4 day cut. Note scale (from 1 to 10 cm on z-axis).

DOI: 10.2312/GFZ.b103-00228

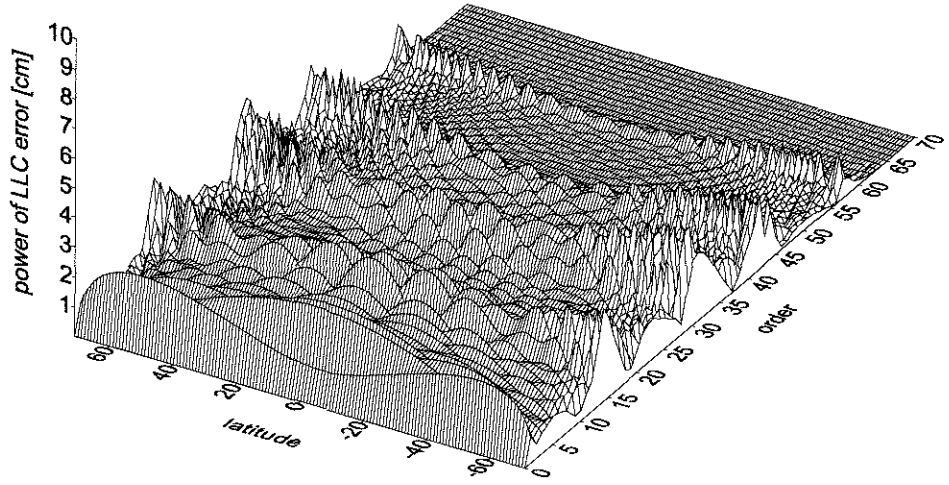

Power of LLC error for Geosat with JGM 3 (70x70), 4 d cut

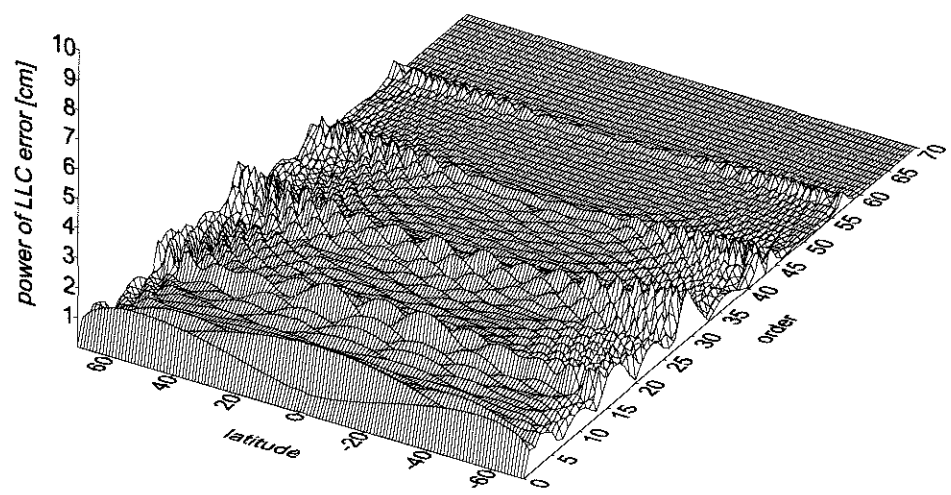

Power of LLC error for Geosat with EGM96 (70x70), 4 d cut

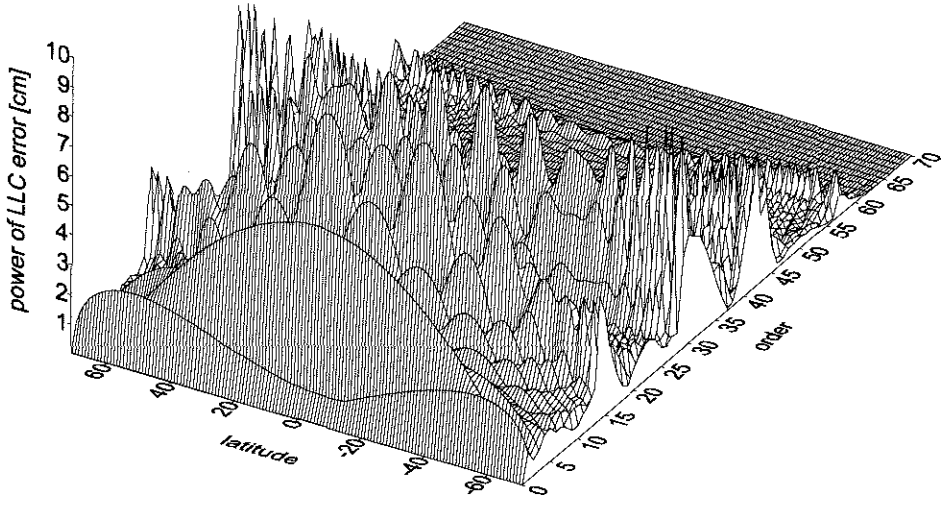

Power of LLC error for Geosat with GRIM5S1 (70x70), 4 d cut

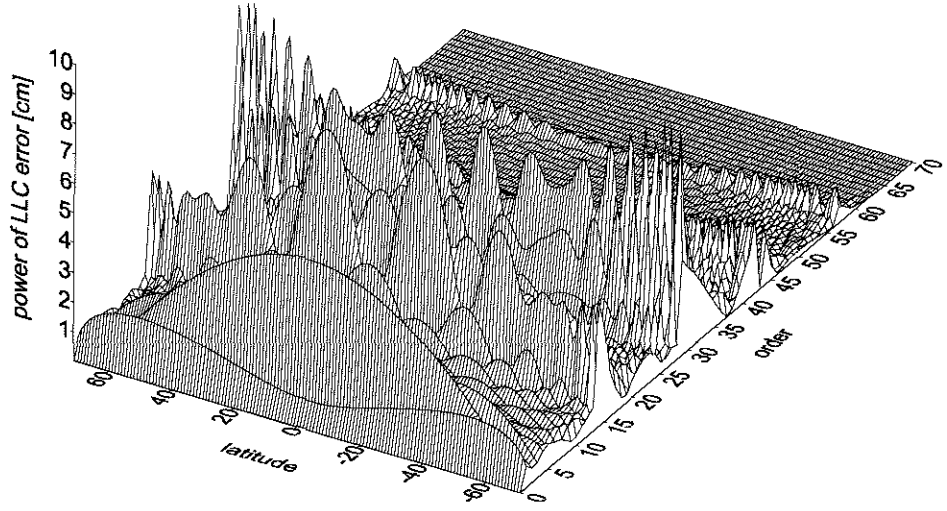

Power of LLC error for Geosat with GRIM5C1 (70x70), 4 d cut

Fig. 18.: Error of latitude lumped coefficients for Geosat with Jgm 3, EGM 96, GRIM5S1 and GRIM5C1 covariances, 4 day cut. Note scale (from 1 to 10 cm on z-axis).

DOI: 10.2312/GFZ.b103-00228

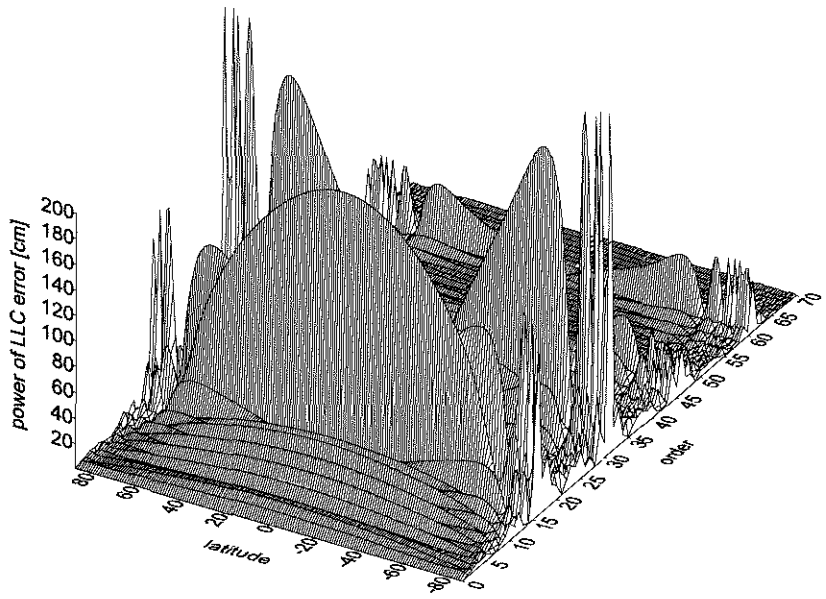

Power of LLC error for CHAMP with JGM 3 (70x70), 4 d cut

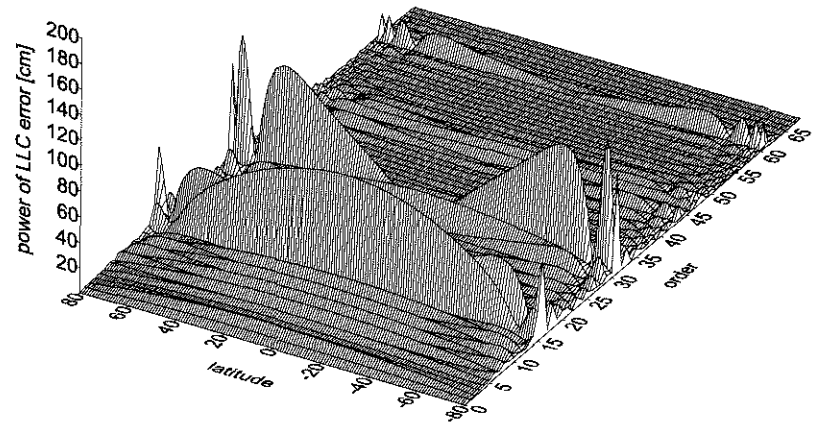

Power of LLC error for CHAMP with EGM 96 (70x70), 4 d cut

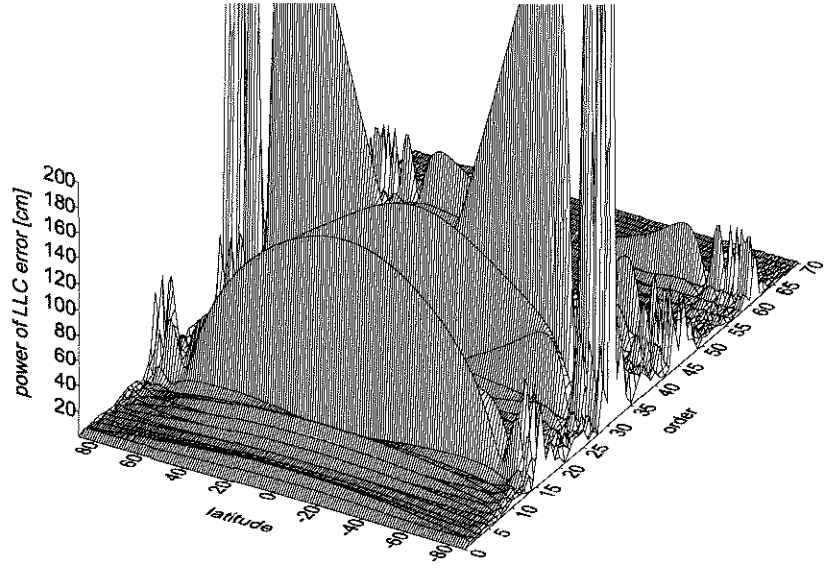

Power of LLC error for CHAMP with GRIM5S1 (70x70), 4 d cut

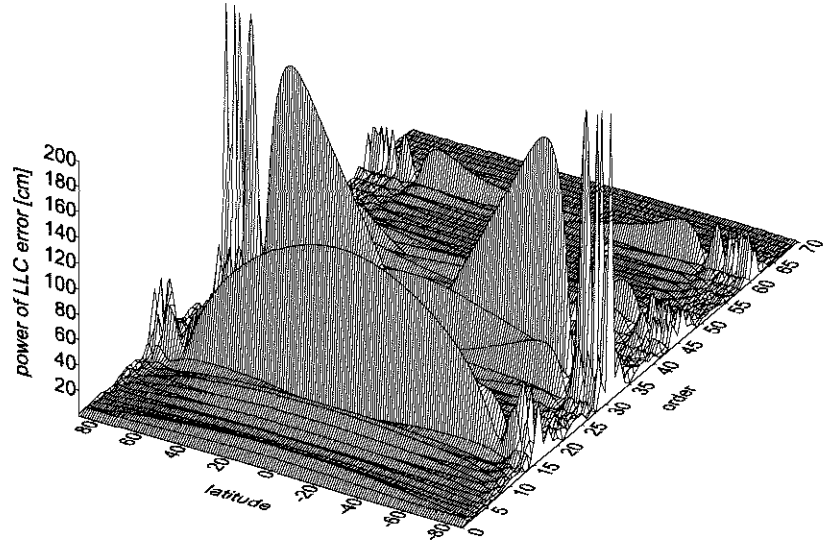

Power of LLC error for CHAMP with GRIM5C1 (70x70), 4 d cut

Fig. 19.: Error of latitude lumped coefficients for CHAMP with Jgm 3, EGM 96, GRIM5S1 and GRIM5C1 covariances, 4 day cut. Note scale (from 1 to 200 cm on z-axis)!

DOI: 10.2312/GFZ.b103-00228

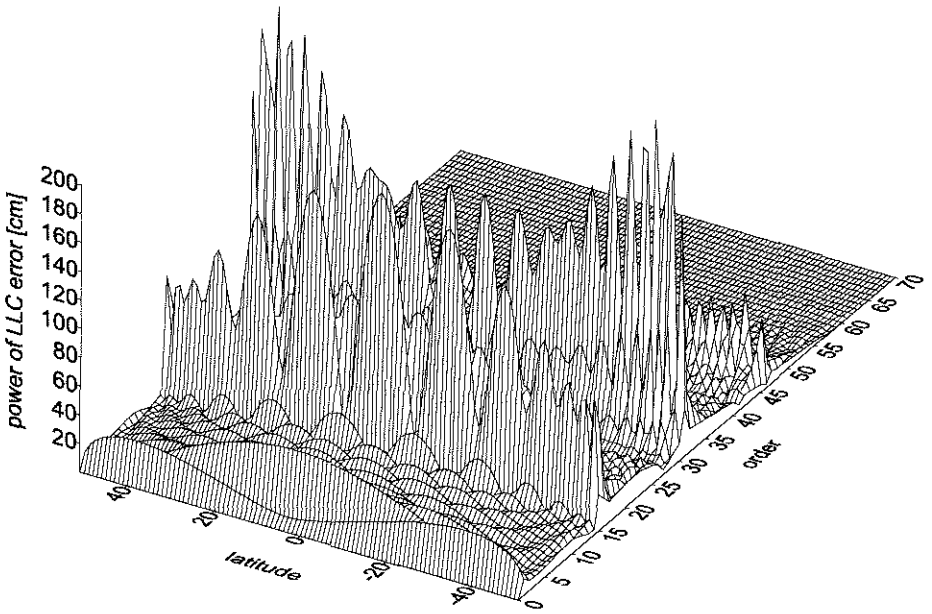

Power of LLC error for GFZ1 with JGM 3 (70x70), 4 d cut

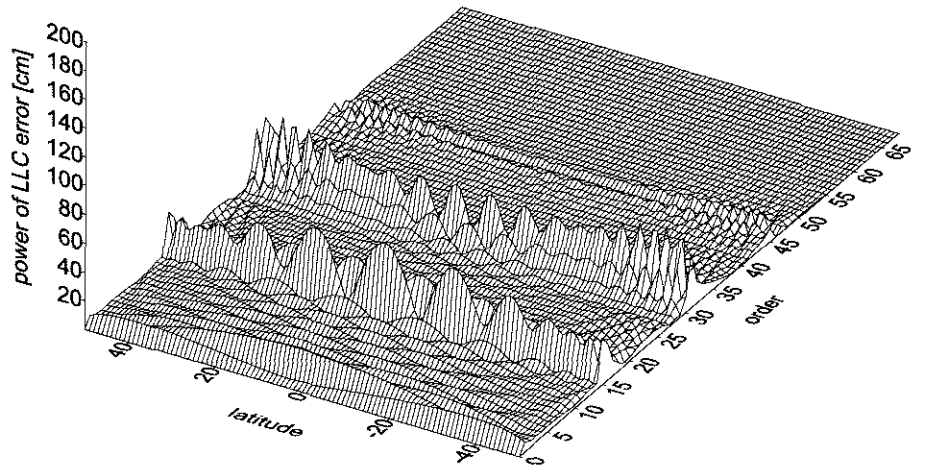

Power of LLC error for GFZ1 with EGM 96 (70x70), 4 d cut

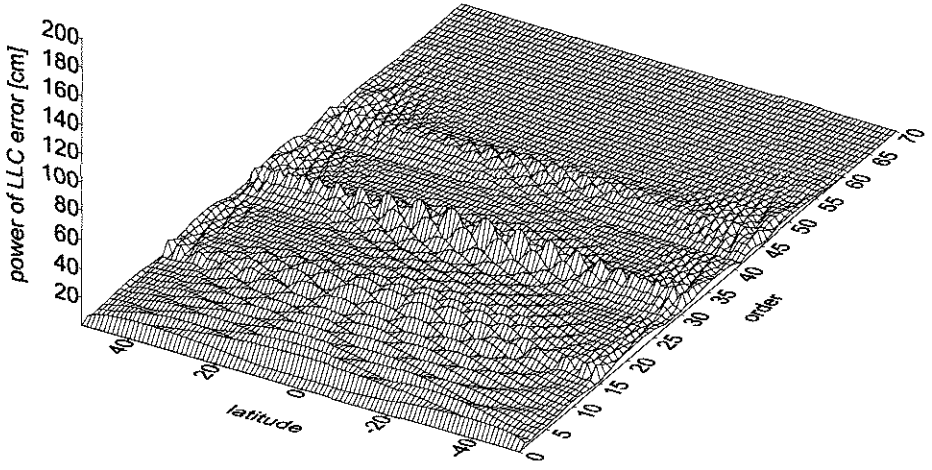

Power of LLC error for GFZ1 with GRIM5S1 (70x70), 4 d cut

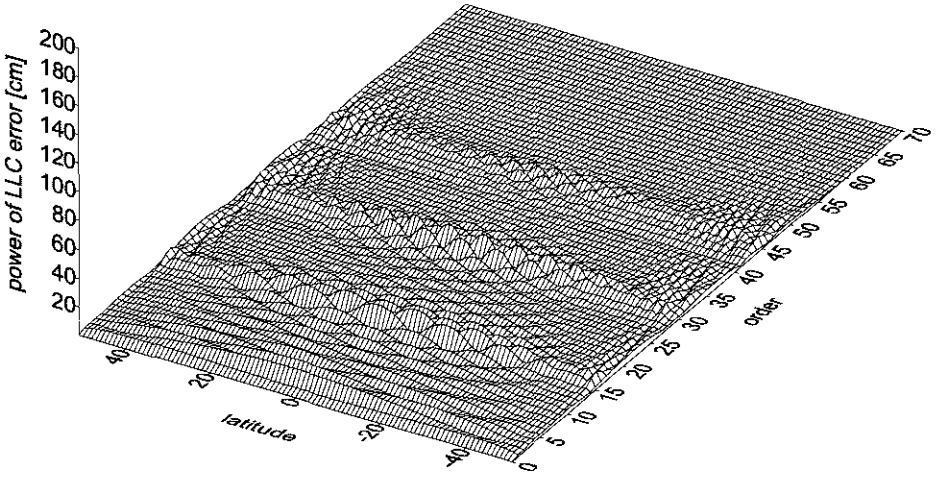

Power of LLC error for GFZ1 with GRIM5C1 (70x70), 4 d cut

Fig. 20.: Error of latitude lumped coefficients for GFZ 1 with JGM 3, EGM 96, GRIM5S1 and GRIM5C1 covariances, 4 day cut.
Note scale (from 1 to 200 cm on z-axis), the same as on Fig.19

DOI: 10.2312/GFZ.b103-00228

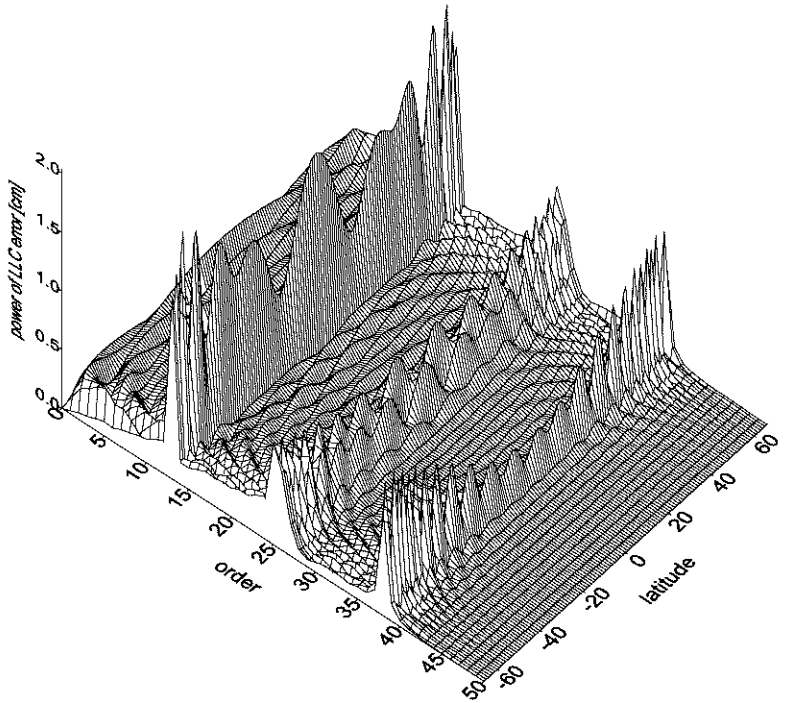

Power of LLC error for TOPEX with JGM 3 (50x50), 10 d cut

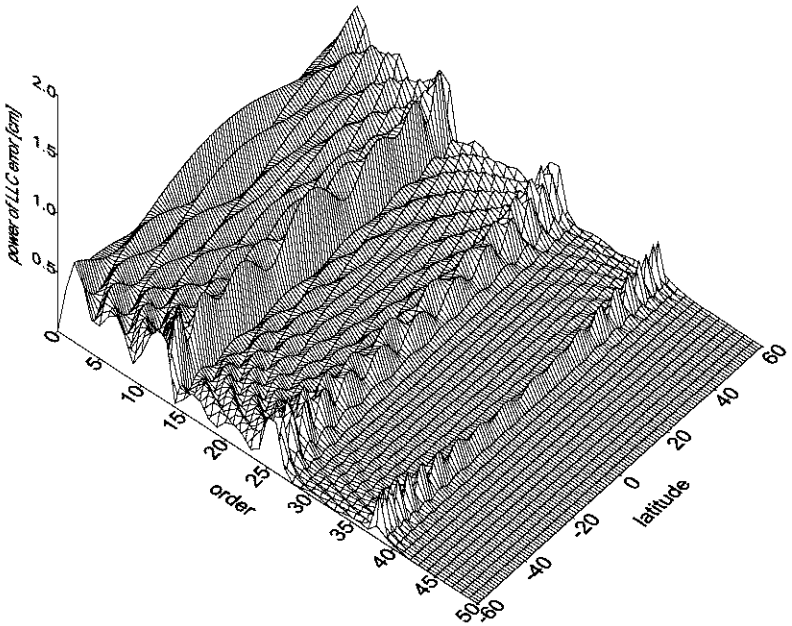

Power of LLC error for TOPEX with EGM 96 (50x50), 10 d cut

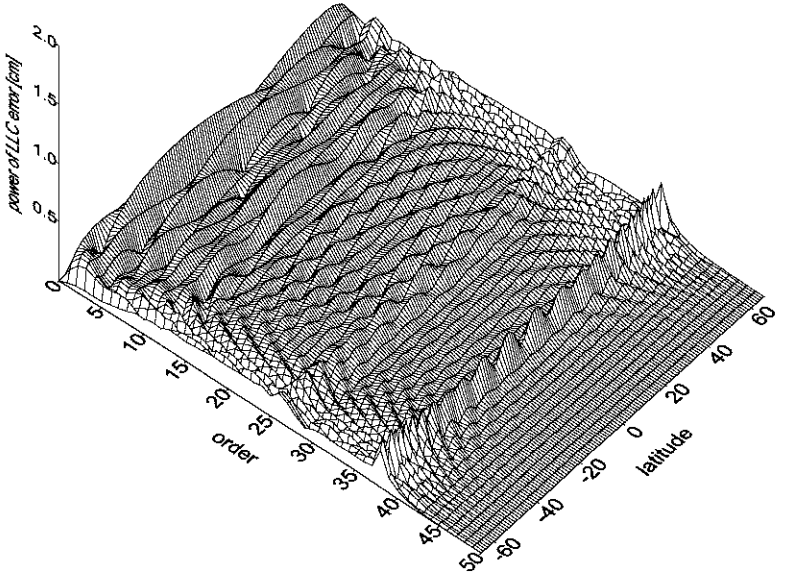

Power of LLC error for TOPEX with GRIM5S1 (50x50), 10 d cut

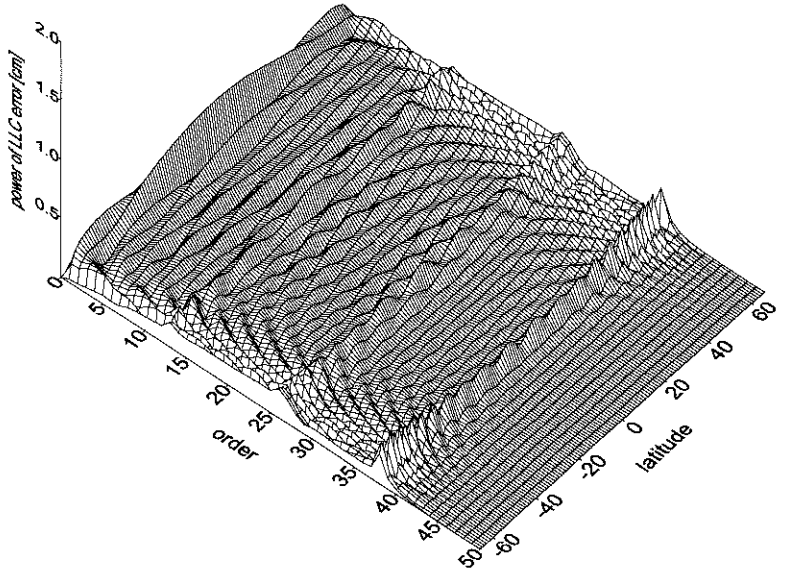

Power of LLC error for TOPEX with GRIM5C1 (50x50), 10 d cut

Fig. 21.: Error of latitude lumped coefficients for TOPEX/Poseidon with Jgm 3, EGM 96, GRIM5S1 and GRIM5C1 covariances, 10 day cut. Note fine scale (from 0 to 1 cm on z-axis).

STR 00/22 German Research Centre for Geosciences
DOI: 10.2312/GFZ.b103-00228

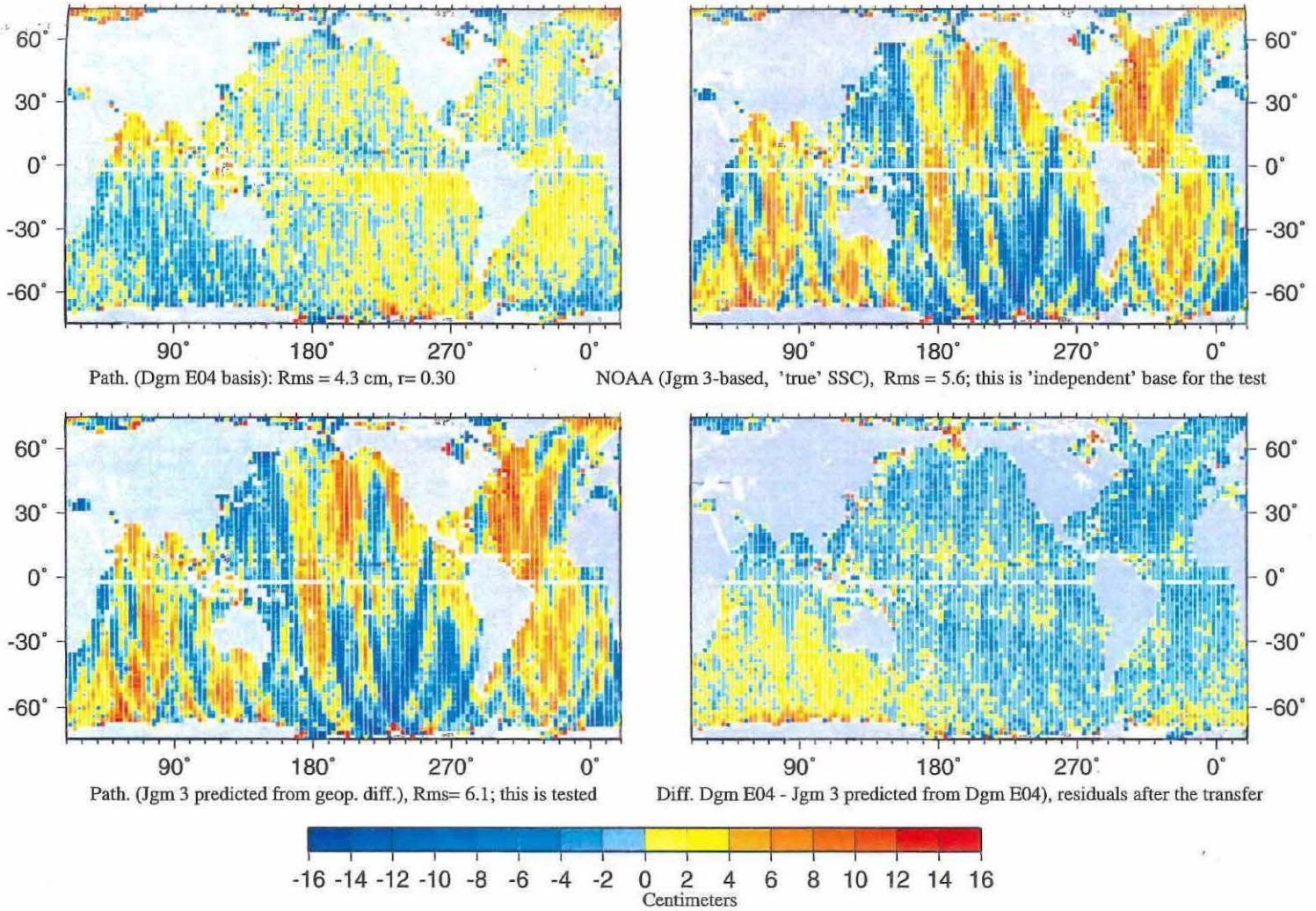

Fig 22. Evaluation of the linear transfer method:
predicted SSC for ERS 1 with Jgm 3 from the original SSC Dgm-E04 -based. A comparison of the prediction with real Jgm 3-based SSC.
Fig 22a (upper left): Original Pathfinder ERS 1 SSC residuals, Dgm-E04 -based.
Fig 22b (upper right): Original Jgm3-based NOAA SSC.
Fig 22c (down left): Predicted Jgm3-based SSC from Dgm-E04 originals, just changing the harmonic geopotential coefficients between the two models.
Fig 22d (down right): The differences (a)-(c) between the Jgm3 original and Jgm3 predicted SSC. *Rms* of the difference is about 2 cm.
Scale: centimeters from -16 to +16.

STR 00/22 German Research Centre for Geosciences
DOI: 10.2312/GFZ.b103-00228

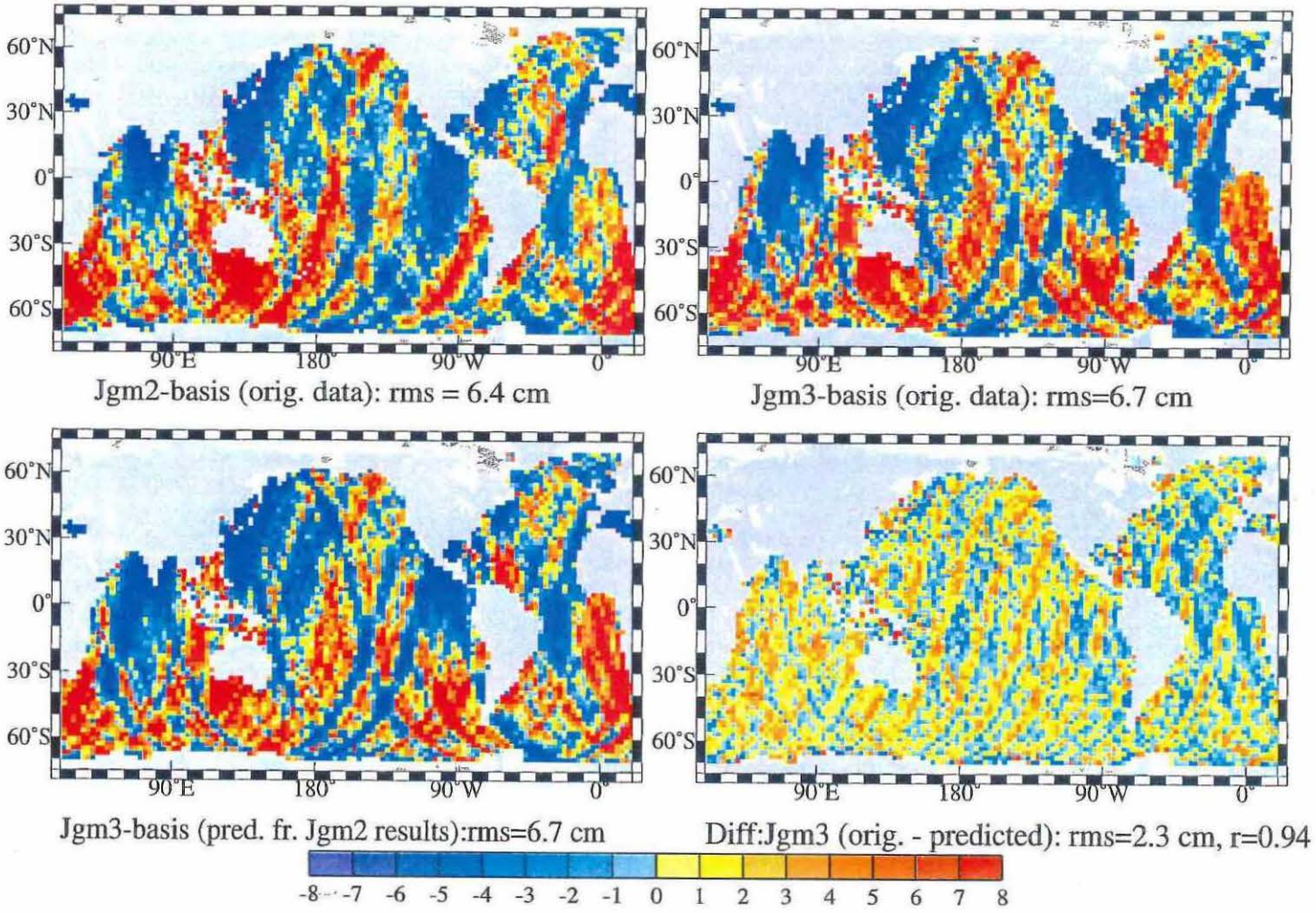

Fig. 23. Evaluation of the linear transfer method: predicted SSC for Geosat (ERM and GM) Jgm3-based from the original 'true' SSC Jgm2-based.
Fig 23a (upper left): Original Jgm2-based NOAA SSC.
Fig 23b (upper right): Original Jgm3-based NOAA SSC.
Fig 23c (down left): Prediction of Jgm3 SSC from Jgm2 originals, just changing the harmonic geopotential coefficients between the two models.
Fig 23d (down right): (b)-(c). The differences between the Jgm3 original "true" SSC residuals and the Jgm3 predicted SSC. *Rms* of the difference is about 2 cm.
Scale: centimeters from -8 to +8.

STR 00/22 German Research Centre for Geosciences
DOI: 10.2312/GFZ.b103-00228

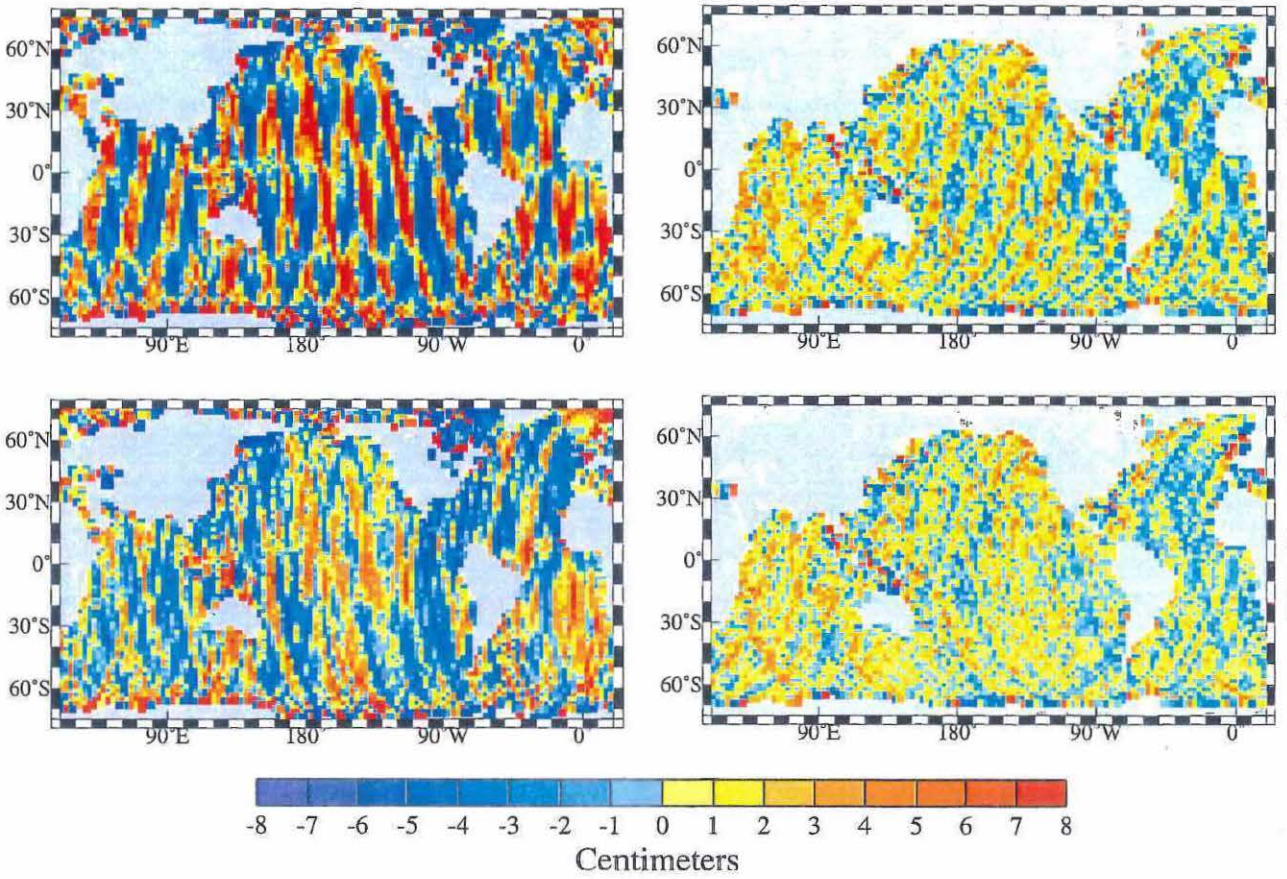

Fig. 24. Fig. 25.

Fig. 24. Evaluation of the linear transfer method, the role of the filter.
(a) GRIM5S1 predicted SSC for ERS 1 from the Jgm3-based originals, with the 4 day cut of orbit perturbations in the transfer. The same information (but in a different scale) is in Fig. 4.
(b) GRIM5S1 predicted SSC for ERS 1 from the Jgm3-based originals, with the 1.3 day cut of orbit perturbations in the transfer.
Scale: centimeters from -8 to +8.

Fig. 25. Evaluation of the linear transfer method, the role of the filter.
(a) GRIM5S1 predicted SSC for Geosat from the Jgm2-based originals, with the 4 day cut of orbit perturbations in the transfer.
(b) GRIM5S1 predicted SSC for Geosat from the Jgm2-based originals, with the 1.3 day cut of orbit perturbations in the transfer.
Scale: centimeters from -8 to +8.

Fig. 26 a-e. Summary of the Student statistics for ERS 1 and Geosat with Jgm 3, GRIM5S1, and GRIM5C1 (to 70x70). Plotted is the ratio r_t, eq. 6 for risk α=1%. Yellow and red areas are the places where the null hypothesis can be rejected (i.e. where are very probably residual systematic errors in the relevant SSC data).
(a) with JGM3-based SSC and JGM3 covariance projections, both with the 4 day cut. The null hypothesis is supported (mainly for Geosat).
(b) with GRIM5S1-transformed SSC and GRIM5S1 covariance projections, both with the 4 day cut. For ERS1, the null hypothesis is rejected, due to many significant values of the ratio r_t in the Pacific area.
(c) with JGM3-based SSC and JGM3 covariance projections, both with the 1.3 day cut. Nearly the same as on (a).
(d) with GRIM5S1-transformed SSC and GRIM5S1 covariance projections, both with the 1.3 day cut. For ERS1, a significant improvement over (b) with the 4 day cut can be seen. The false resonant waves with the orbit perturbations between 4 and 1.3 days, modulated by the linear transfer in the case (b), are here nearly removed. The null hypothesis might be still accepted, but some doubths are about Geosat in the Pacific ocean.
(e) with GRIM5C1-transformed SSC and GRIM5C1 covariance projections, both with the 1.3 day cut. We are inclined to reject the null hypothesis.

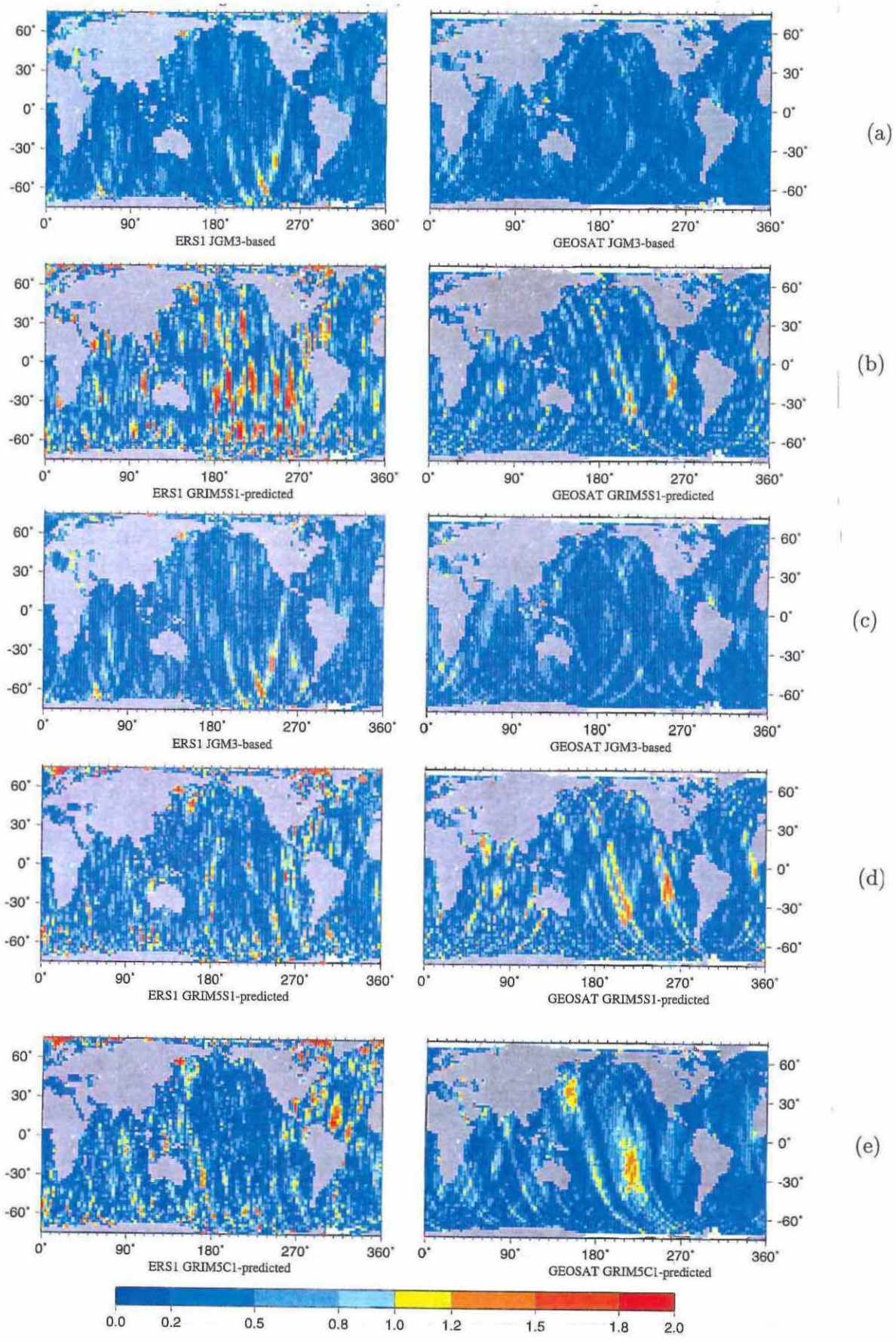

Fig. 26 a-e.

STR 00/22 German Research Centre for Geosciences
DOI: 10.2312/GFZ.b103-00228

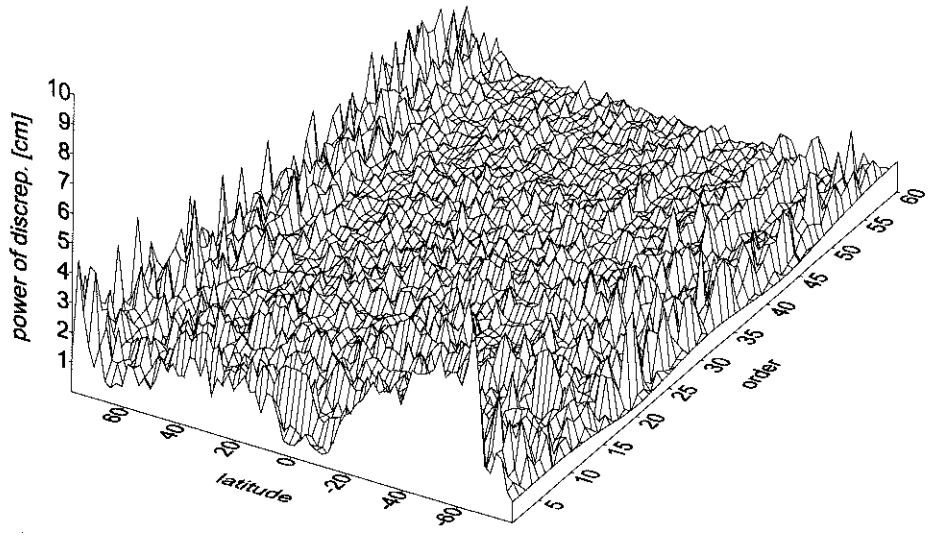

Power of LLC discrepancies of ERS 1 SSC JGM 3-based

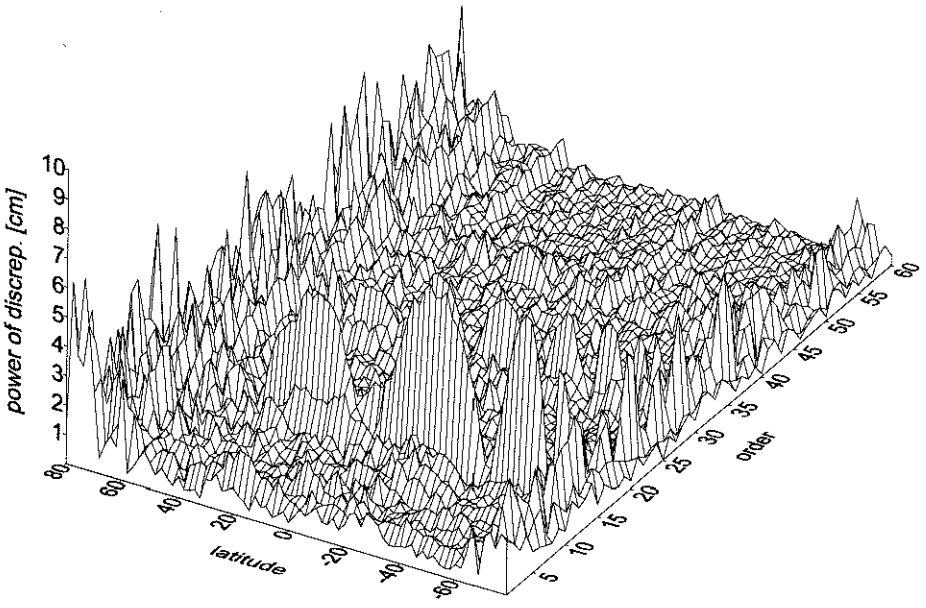

Power of LLC discrepancies of ERS 1 predicted SSC GRIM5S1- based

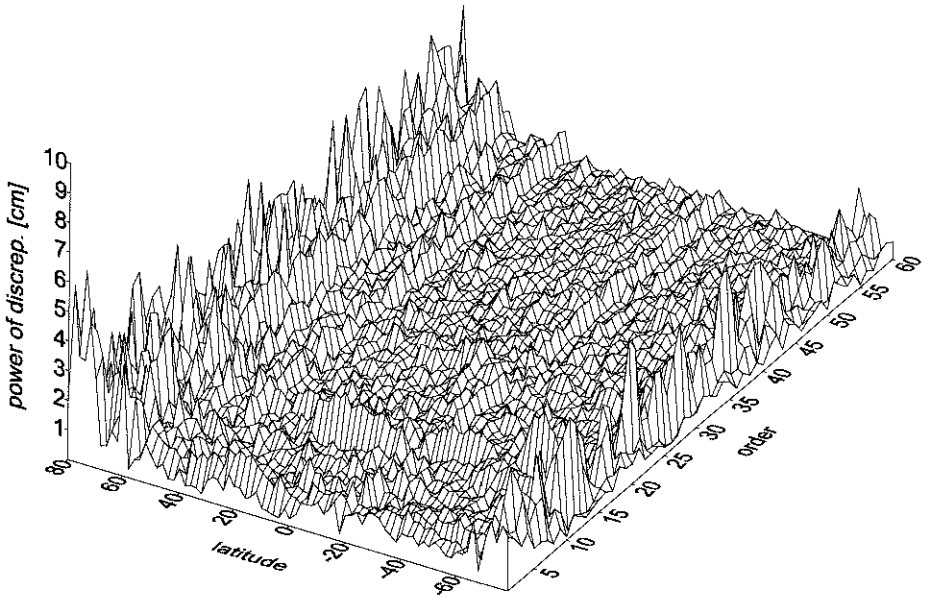

Power of LLC discrepancies of ERS 1 predicted SSC GRIM5C1-based

Fig. 27.: Powers of LLC discrepancies of ERS 1 SSC, JGM 3-based, GRIM5S1 and GRIM5C1-predicted.

STR 00/22 German Research Centre for Geosciences
DOI: 10.2312/GFZ.b103-00228

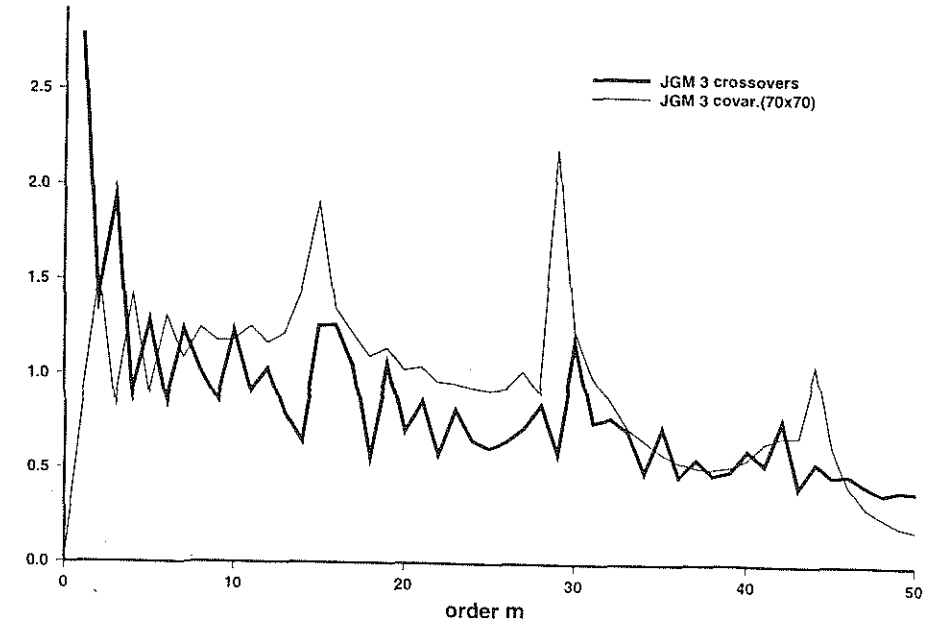

RMS of power of LLC discrep./errors for ERS1, JGM 3, 1.3d cut

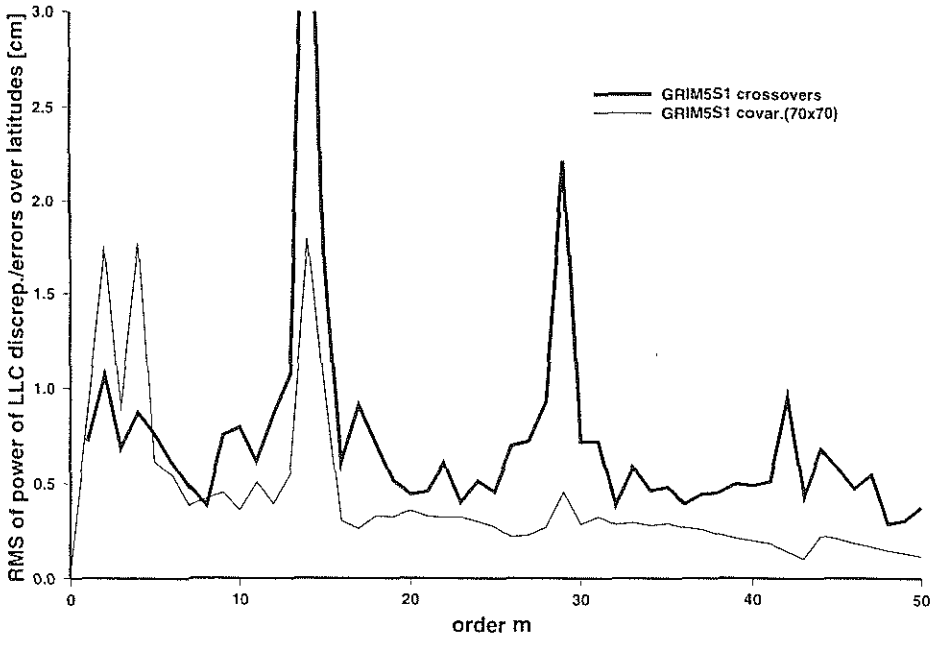

RMS of power of LLC discrep./errors for ERS1, GRIM5S1, 1.3d cut

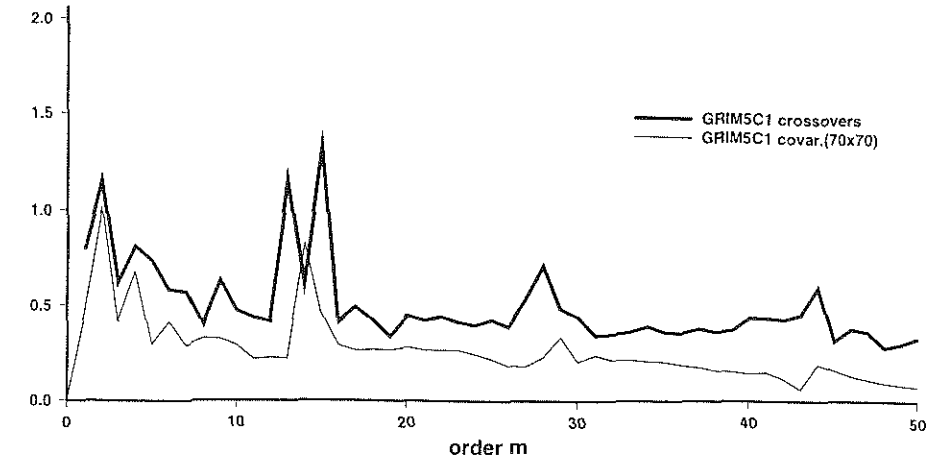

RMS of power of LLC discrep./errors for ERS1, GRIM5C1, 1.3d cut

Fig. 28. Comparison of rms of powers of LLC discrepancies and errors over latitudinal belts from 20 to -60 deg (southern hemisphere) of Ers 1 SSC, JGM 3-based, GRIM5-S1 and GRIM5-C1-predicted.

STR 00/22 German Research Centre for Geosciences
DOI: 10.2312/GFZ.b103-00228

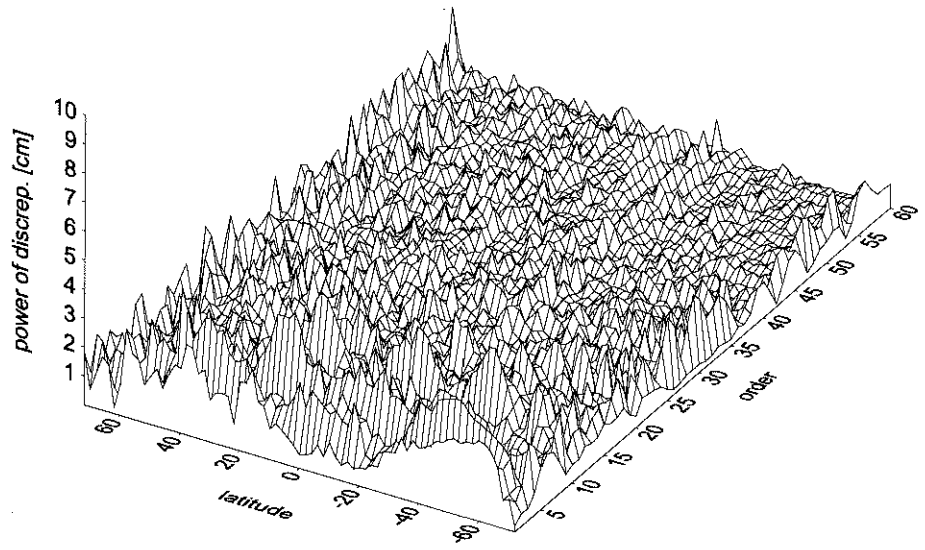

Power of LLC discrepancies of GEOSAT SSC JGM 3-based

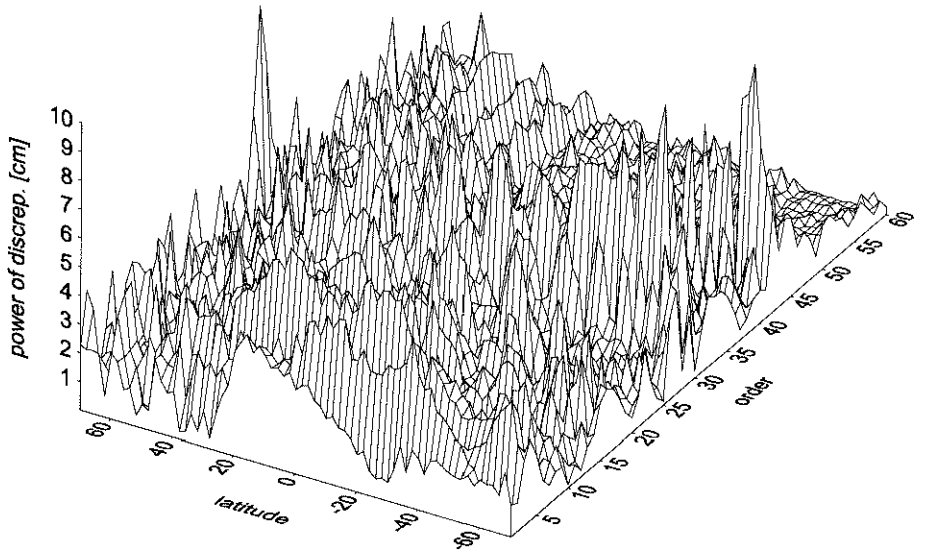

Power of LLC discrepancies of GEOSAT predicted SSC GRIM5S1-based

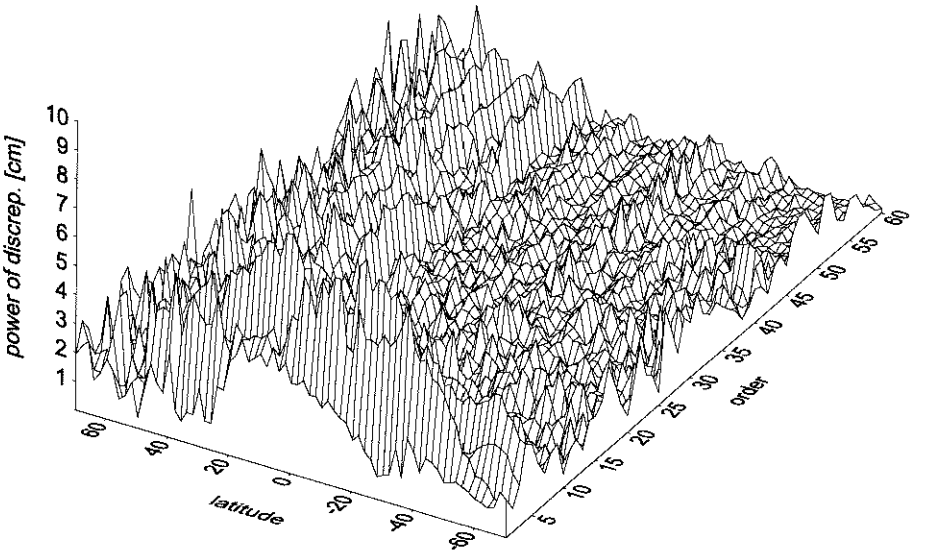

Power of LLC discrepancies of GEOSAT predicted SSC GRIM5C1-based

Fig. 29.: Powers of LLC discrepancies of Geosat SSC, Jgm 3-based, GRIM5S1 and GRIM5C1-predicted.

DOI: 10.2312/GFZ.b103-00228

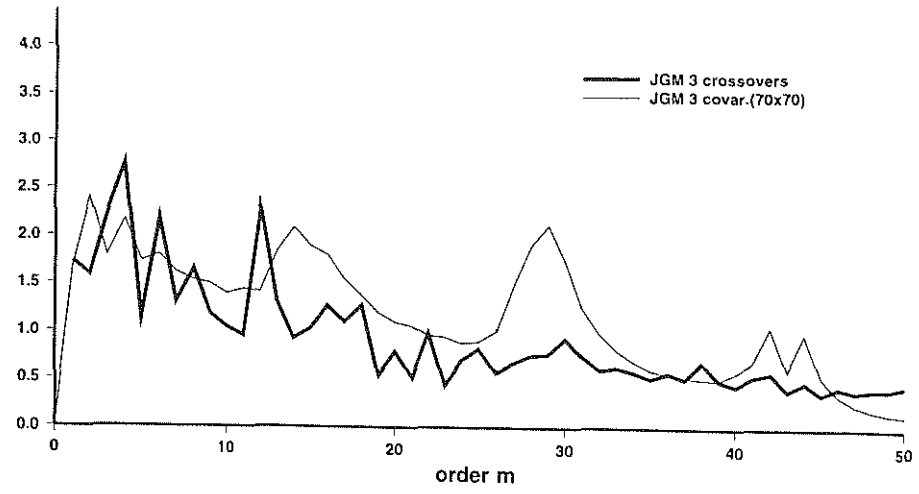

RMS of power of LLC discrep./errors for Geosat, JGM 3

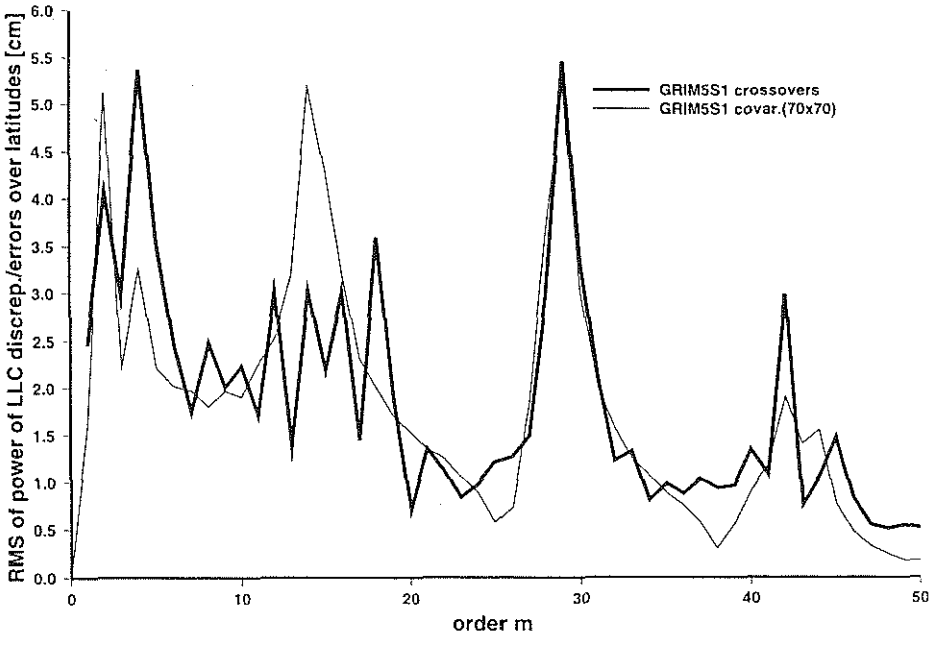

RMS of power of LLC discrep./errors for Geosat, GRIM5S1

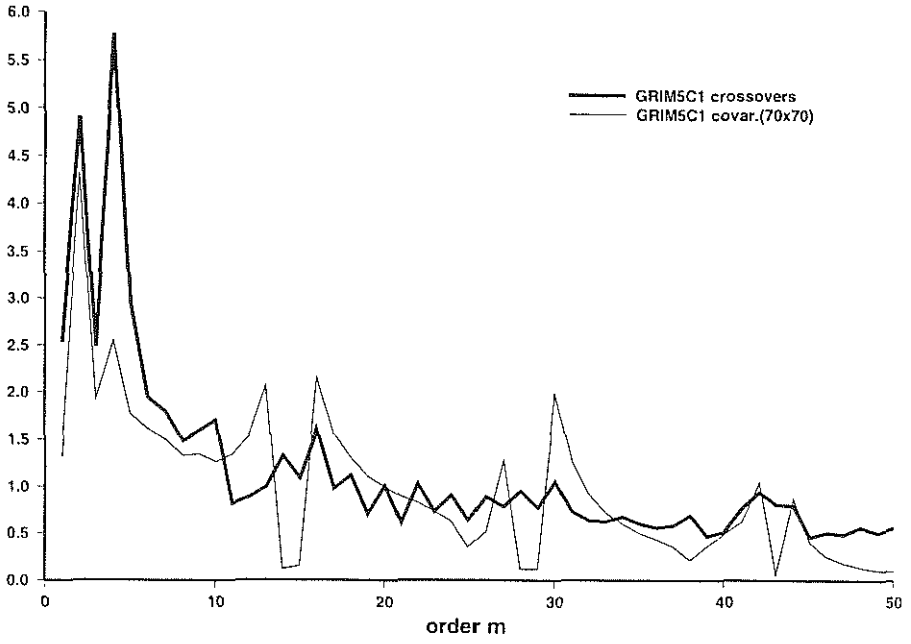

RMS of power of LLC discrep./errors for Geosat, GRIM5C1

Fig. 30. Comparison of rms of powers of LLC discrepancies and errors over latitudinal belts from 20 to -60 deg (southern hemisphere) of Geosat SSC, JGM 3-based, GRIM5-S1 and GRIM5-C1-predicted.

DOI: 10.2312/GFZ.b103-00228

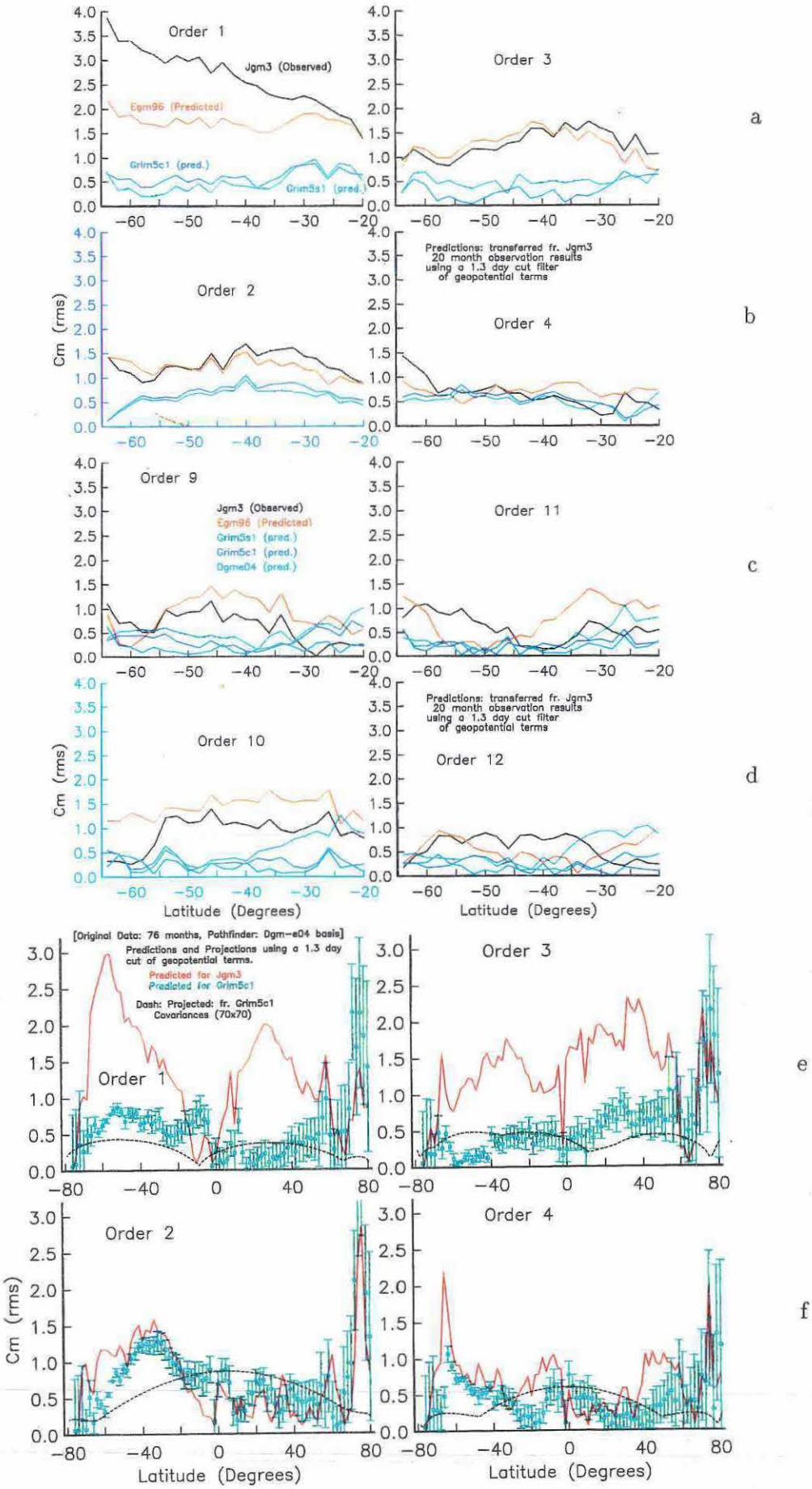

Fig. 31. Few examples of the observed and predicted LLC errors for ERS 1 SSC (plots a,b,c,d) and for the combination of ERS 1 and 2 (e, f) with various covariances (Jgm 3, , EGM 96, Dgm E04, GRIM5S1, and GRIM5C1, always to degree and order 70x70) for few selected orders. The predictions are computed with the 1.3 day cut of orbit perturbations.

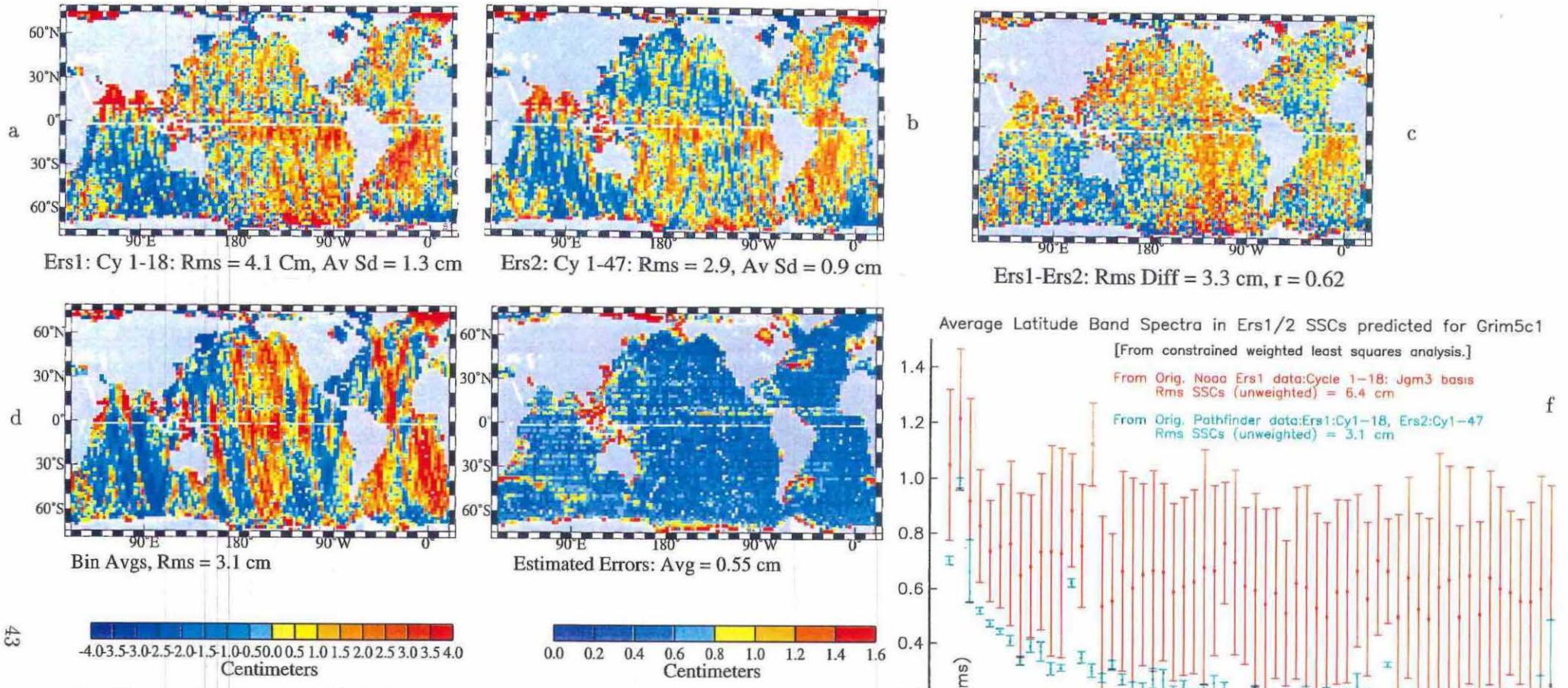

Fig. 32. (a, b, c) Averaged ERS 1 and 2 crossovers from NASA Pathfinder Altimetry, Dgm E04 based, from left to right, for ERS 1 only, ERS 2 only and the difference. Note the *rms* values and correlation coefficient r between the ERS 1 and ERS 2 files. (d, e) Averaged ERS 1 and 2 crossovers from the NASA Pathfinder altimetry, but linearly transformed to GRIM5C1 base. Note the scales for the SSC residuals (d) and their formal standard deviations (e) different from those for the ERS 1 data on Fig. 4a–d or 6a, and 4e,f, respectively. (f) Averaged latitude band spectra in ERS 1 and 2 SSC predicted (transformed) for GRIM5C1 model, over latitudes for the individual orders of harmonics. The original NOAA ERS 1 data alone has much higher inaccuracy and *rms* value in comparison with the NASA Pathfinder data for both ERS 1 (18 first cycles) and ERS 2 (47 cycles).

STR 00/22 German Research Centre for Geosciences
DOI: 10.2312/GFZ.b103-00228

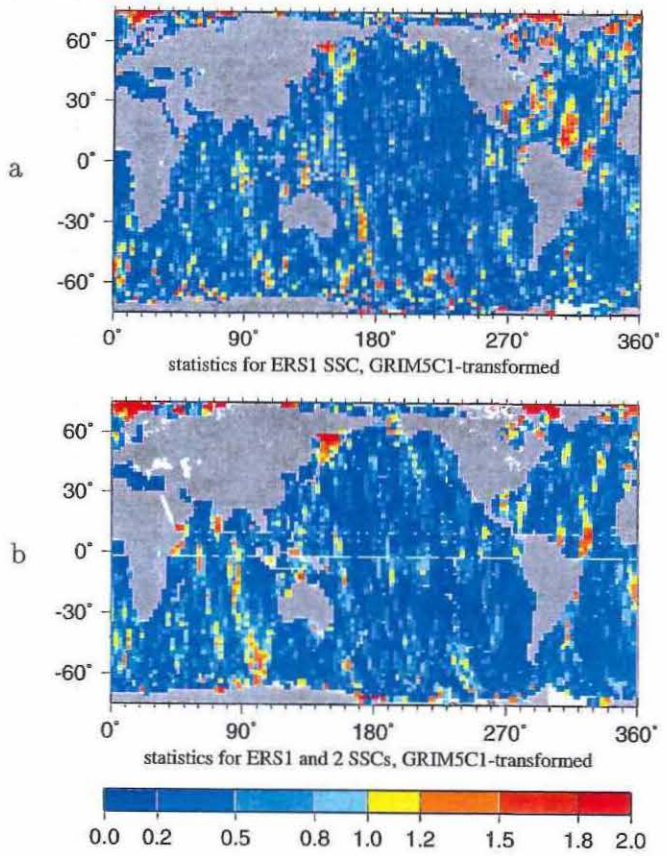

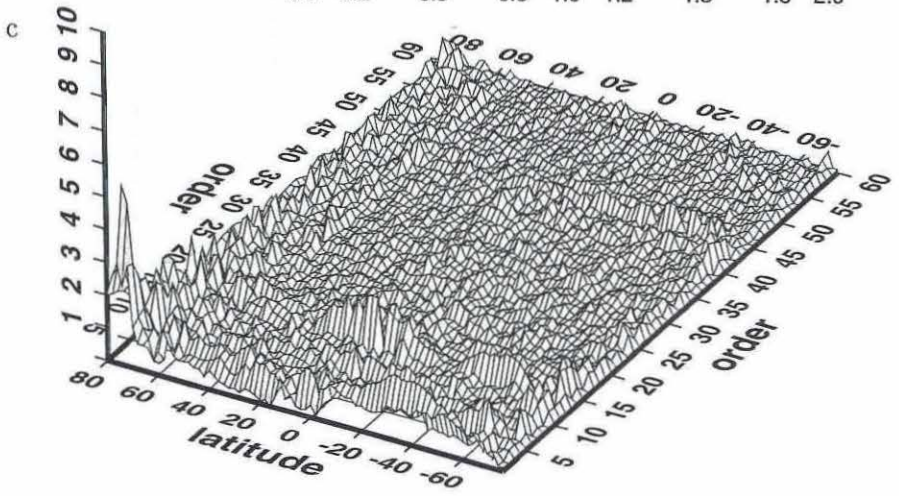

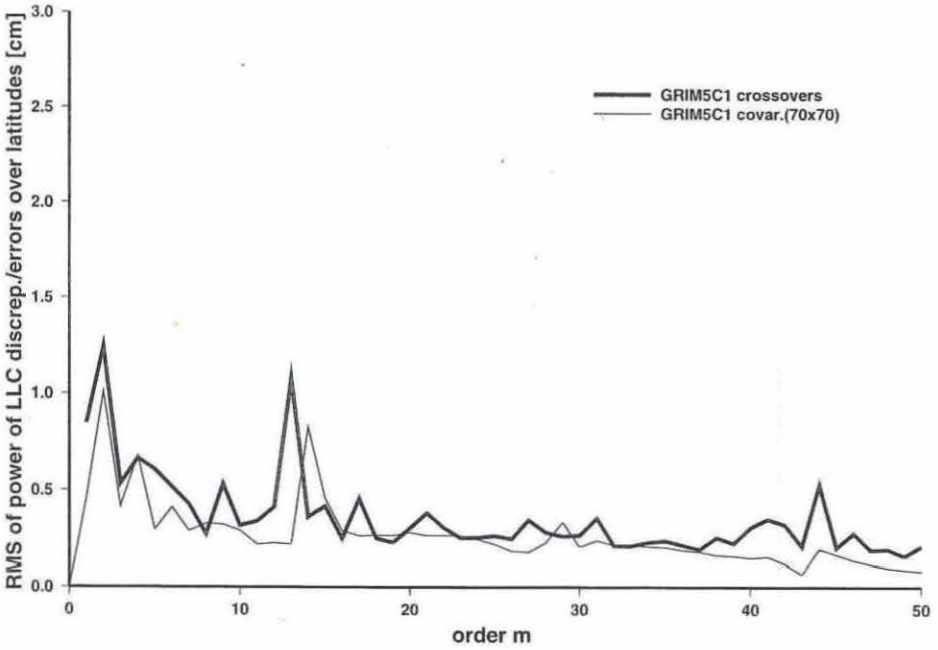

Fig. 33. (a, b) Student statistics for ERS 1 and ERS 1 plus ERS 2 SSC, GRIM5C1 transformed, 1.3 day cut. Fig. 33 a is the same as Fig. 26 e (left). (c) Power of the LLC discrepancies of ERS 1 and 2 SSC, GRIM5C1-predicted, 1.3 d cut. Compare with Fig. 27 c. Scale on z axis [cm]. (d) RMS of powers of LLC discrepancies and error over latitudinal belts from 20 to -60 deg, using the combination of ERS 1 and 2 SSC residuals. To be compared to Fig. 28 c.

STR 00/22 German Research Centre for Geosciences
DOI: 10.2312/GFZ.b103-00228